CHAPTER 4
EVAPORATION

W. James Shuttleworth*
Hydrological Processes Division
Institute of Hydrology
Wallingford, United Kingdom

4.1 INTRODUCTION

Evaporation occurs when water is converted into water vapor. The rate is controlled by the availability of energy at the evaporating surface, and the ease with which water vapor can diffuse into the atmosphere. Different physical processes are responsible for the diffusion, but the physics of water vapor loss from open-water surfaces and from soils and crops is essentially identical. In this chapter evaporation is defined as *the rate of liquid water transformation to vapor from open water, bare soil, or vegetation with soil beneath.* Unless otherwise stated, this rate is in millimeters of evaporated water per day. In the case of vegetation growing in soil, transpiration is defined as *that part of the total evaporation which enters the atmosphere from the soil through the plants.*

The rate of evaporation has traditionally been estimated using meteorological data from climate stations located at particular points within a region, and it has been assumed that the evaporating area is sufficiently small that the evaporation has no effect on regional climate or air movement. In reality, this simplified approach approximates a more complex situation in which local evaporation is a function of both local climate and regional air movement. With the advance of scientific studies of evaporation and the availability of remotely sensed measurements of regional variables such as temperature and radiation, it is to be expected that eventually evaporation estimation for local areas will be made a function of both local and regional variables; but for the moment, such estimates are possible only on intensively instrumented experimental sites.

4.1.1 Standard Evaporation Rates

Two standard evaporation rates are defined, *potential evaporation* and *reference crop evaporation,* and used as the basis for evaporation estimates. These rates are concep-

*Now at Department of Hydrology and Water Resources, University of Arizona, Tucson, Arizona.

tual in the sense that they represent idealized situations. In particular they ignore the fact that meteorological parameters near the surface are influenced by upwind surface energy exchange; that is, evaporation introduces water into the air and can remove energy from it, which changes the atmospheric humidity deficit and may alter the evaporation at downwind locations.

Potential Evaporation E_0 (in Millimeters per Day). Potential evaporation is here defined as *the quantity of water evaporated per unit area, per unit time from an idealized, extensive free water surface under existing atmospheric conditions.* This is a conceptual entity which measures the meteorological control on evaporation from an open water surface.

Reference Crop Evaporation E_{rc} (in Millimeters per Day). Reference crop evaporation is here defined as *the rate of evaporation from an idealized grass crop with a fixed crop height of 0.12 m, an albedo of 0.23, and a surface resistance of 69 s m⁻¹.* In terms of its evaporation rate, such a crop closely resembles previous definitions of a reference crop, namely, an extensive surface of short green grass cover of uniform height, actively growing, completely shading the ground, and not short of water.

4.2 PHYSICS OF EVAPORATION AND TRANSPIRATION

4.2.1 Surface Exchanges

Latent Heat. The molecules in liquid water are held close together by attractive intermolecular forces. In water vapor the molecules are at least ten times farther apart than in the liquid phase, so the intermolecular force is very much smaller. During evaporation, separation between molecules increases greatly, work is done against the attractive intermolecular force, and energy is absorbed. The energy required is called the *latent heat of vaporization of water* λ, and it decreases slightly with increasing water temperature since the initial separation of the molecules increases with temperature. If T_s is the surface temperature of the water in degrees Celsius, the latent heat of vaporization is given[51] by

$$\lambda = 2.501 - 0.002361\ T_s \qquad \text{MJ kg}^{-1} \tag{4.2.1}$$

which means about 2.5 million joules are required to evaporate a kilogram of water, where the joule is the standard SI unit of energy.

Water Molecule Movement between Water Surfaces and Air. Natural evaporation occurs by exchange of water molecules between air and a free water surface. This water surface could be a lake or a river, or inside plant leaves, adhering to soil particles, or on soil or vegetation surfaces during or just after rain.

Figure 4.2.1 illustrates the exchange of water molecules between liquid and vapor. Some of the vapor molecules hitting the surface rebound, but the capture rate of molecules by the surface is proportional to their rate of surface collision, and therefore to e, the vapor pressure adjacent to the water surface. A molecule must have a minimum energy if it is to leave the surface, and the number of such molecules is related to the surface temperature.

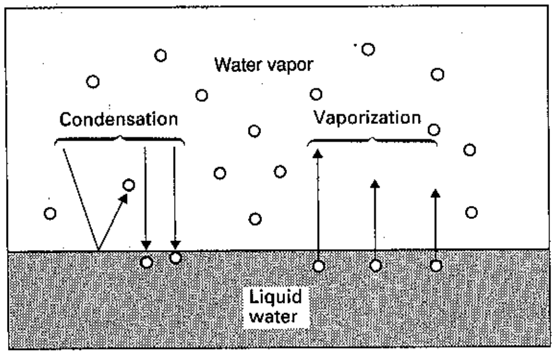

FIGURE 4.2.1 Molecular exchange between liquid water and water vapor. Not all the molecules hitting the surface are captured, but some condense at a rate which is proportional to the vapor pressure of the moist air: molecules with enough energy vaporize at a rate determined by the surface temperature.

Saturated Vapor Content of Air. Evaporation is the difference between two rates,[102] a *vaporization rate* determined by temperature, and a *condensation rate* determined by vapor pressure. If molecules can diffuse away from the surface, vapor pressure remains low, and the difference between these two rates is positive, so evaporation continues. If, on the other hand, the air above the water is thermally insulated and enclosed, the vapor pressure increases until the rates of vaporization and condensation are equal and there is no more evaporation. The air is then said to be *saturated.* At a given temperature this equilibrium occurs for a particular vapor pressure e_s. This is called the *saturated vapor pressure* and is related to temperature; if e_s is in kilopascals and T is in degrees Celsius, an approximate equation[118] is

$$e_s = 0.6108 \exp\left(\frac{17.27\ T}{237.3 + T}\right) \qquad \text{kPa} \tag{4.2.2}$$

It is important in building physically based models of evaporation that not only is e_s a known function of temperature, but so is Δ, the gradient of this function, de_s/dT. This gradient is given by

$$\Delta = \frac{4098\ e_s}{(237.3 + T)^2} \qquad \text{kPa °C}^{-1} \tag{4.2.3}$$

Table 4.2.1 lists values of e_s and Δ as a function of temperature.

Sensible Heat. A portion of the radiant energy input to the earth's surface is not used for evaporation; rather it warms the atmosphere in contact with the ground and then moves upward. We speak of the associated flow of energy as "sensible" heat flux because it changes air temperature, a property of air that can be measured or sensed. The temperature change is proportional to the product $(c_p\rho_a)$, where ρ_a is the density of air and c_p is the specific heat of air at constant pressure, taken as 1.01 kJ kg⁻¹ K⁻¹. The density of (moist) air can be calculated from the ideal gas laws, but it is ade-

TABLE 4.2.1 Temperature Dependence of Saturated Vapor Pressure e_s, Its Temperature Gradient Δ, Together with the Psychrometric Constant at Standard Atmospheric Pressure

Temperature, °C	Saturated vapor pressure e_s, kPa	Gradient of saturated vapor pressure Δ, kPa °C^{-1}	Psychrometric constant γ, kPa °C^{-1}
0	0.611	0.044	0.0654
1	0.657	0.047	0.0655
2	0.706	0.051	0.0656
3	0.758	0.054	0.0656
4	0.814	0.057	0.0657
5	0.873	0.061	0.0658
6	0.935	0.065	0.0659
7	1.002	0.069	0.0659
8	1.073	0.073	0.0660
9	1.148	0.078	0.0660
10	1.228	0.082	0.0661
11	1.313	0.087	0.0661
12	1.403	0.093	0.0662
13	1.498	0.098	0.0663
14	1.599	0.104	0.0663
15	1.706	0.110	0.0664
16	1.819	0.116	0.0665
17	1.938	0.123	0.0665
18	2.065	0.130	0.0666
19	2.198	0.137	0.0666
20	2.339	0.145	0.0667
21	2.488	0.153	0.0668
22	2.645	0.161	0.0668
23	2.810	0.170	0.0669
24	2.985	0.179	0.0670
25	3.169	0.189	0.0670
26	3.363	0.199	0.0671
27	3.567	0.209	0.0672
28	3.781	0.220	0.0672
29	4.007	0.232	0.0673
30	4.244	0.243	0.0674
31	4.494	0.256	0.0674
32	4.756	0.269	0.0675
33	5.032	0.282	0.0676
34	5.321	0.296	0.0676
35	5.625	0.311	0.0677
36	5.943	0.326	0.0678
37	6.277	0.342	0.0678
38	6.627	0.358	0.0679
39	6.994	0.375	0.0670

quately estimated from

$$\rho_a = 3.486 \frac{P}{275 + T} \quad \text{kg m}^{-3} \tag{4.2.4}$$

where P is the atmospheric pressure in kPa and T is air temperature in degrees Celsius.

The sensible heat flux, or heat flow per unit area H, is commonly upward from the ground during the day, but it is usually downward at night to support radiant energy loss from the land surface. Locally the flux of sensible heat can be downward during the day if the vegetation is wet and evaporation is rapid.

4.2.2 Radiation Balance at Land Surfaces

In the absence of restrictions due to water availability at the evaporative surface, the amount of radiant energy captured at the earth's surface is the dominant control on regional evaporation rates. As a monthly average, the radiant energy at the ground may be the most "portable" meteorological variable involved in evaporation estimation, in the sense that it is driven by astronomical rather than local climate conditions. Understanding surface radiation balance, and how to quantify it, is therefore crucial to understanding and quantifying evaporation.

Net Short-Wave Radiation. Figure 4.2.2 illustrates the radiation balance at the earth's surface. The sun is the main source of radiant energy. It is equivalent to a radiator of about 6000°C, but the input of extraterrestrial short-wave radiation S_0 is modified by absorption by atmospheric gases, particularly water vapor, through scattering by air molecules and dust particles in clear sky conditions, and additionally by clouds when these are present. Much of the radiation has short wavelengths, 0.3 to

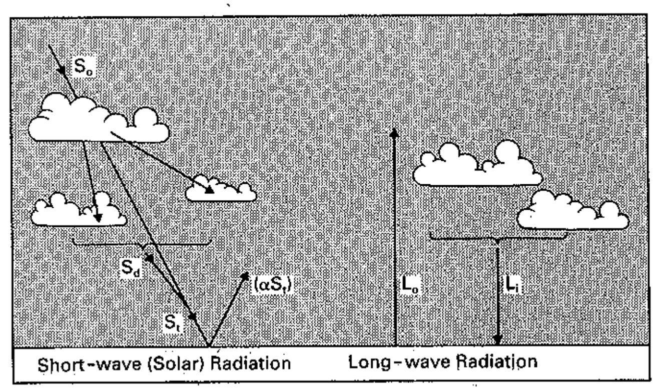

FIGURE 4.2.2 Radiation balance at the earth's surface. A proportion S_t of the solar radiation incident at the top of the atmosphere S_0 reaches the ground, some S_d indirectly after scattering by air and cloud. A proportion α, the albedo, is reflected. Outward long-wave radiation L_0 is partly compensated by incoming long-wave radiation L_i. S_t is typically 25 to 75 percent of S_0, while S_d can vary between 15 and 100 percent of S_t: both these proportions are influenced by cloud cover. α is typically 0.23 for land surfaces and 0.08 for water surfaces.

3.0 μm, the spectrum varying with the fraction of the total short-wave energy input S_t reaching the ground in the direct solar beam. Some of the short-wave radiation S_d reaches the surface in a diffuse, i.e., multidirectional form after scattering by atmospheric particles and clouds. This fraction is typically 15 to 25 percent in clear sky conditions but approaches 100 percent in overcast conditions.

Part of the short-wave radiation is reflected. The reflection coefficient or short-wave *albedo* α depends on transient features, such as the direction of the solar beam, and the proportion of diffuse radiation, but it also changes with land cover, since taller vegetation usually reflects less solar radiation than does shorter vegetation. The scientific literature reporting measured short-wave albedo is extensive, and reported values vary greatly. However, Table 4.2.2 gives the author's recommendation on plausible values of albedo for broad land cover classes. The value $\alpha = 0.23$ is a good overall average value for grassland and a range of agricultural crops, and $\alpha = 0.08$ is a reasonable value for open water surfaces.

The *net short-wave radiation* S_n is that portion of the incident short-wave radiation captured at the ground taking into account losses due to reflection, and is given by

$$S_n = S_t(1-\alpha) \qquad \text{MJ m}^{-2}\text{ day}^{-1} \tag{4.2.5}$$

Solar radiation is measured in specialized agrometeorological stations with radiometers. These instruments require careful calibration and maintenance, however, and measured solar radiation data are usually not available at standard stations. The total incoming short-wave radiation can in most cases be estimated[16] from measured sunshine hours according to the following empirical relationship:

$$S_t = \left(a_s + b_s\frac{n}{N}\right)S_0 \qquad \text{MJ m}^{-2}\text{ day}^{-1} \tag{4.2.6}$$

where a_s = fraction of extraterrestrial radiation S_0 on overcast days ($n = 0$)
$a_s + b_s$ = fraction of extraterrestrial radiation S_0 on clear days
n/N = cloudiness fraction
n = bright sunshine hours per day, h
N = total day length, h
S_0 = extraterrestrial radiation, MJ m^{-2} day^{-1}

TABLE 4.2.2 Plausible Values for Daily Mean Short-Wave Solar Radiation Reflection Coefficient (Albedo) for Broad Land Cover Classes

Land cover class	Short-wave radiation reflection coefficient α
Open water	0.08
Tall forest	0.11–0.16
Tall farm crops (e.g., sugarcane)	0.15–0.20
Cereal crops (e.g., wheat)	0.20–0.26
Short farm crops (e.g., sugar beet)	0.20–0.26
Grass and pasture	0.20–0.26
Bare soil	0.10 (wet)–0.35 (dry)
Snow and ice	0.20 (old)–0.80 (new)

Note: Albedo can vary widely with time of day, season, latitude, and cloud cover.
In the absence of knowledge on crop cover the value $\alpha = 0.23$ is recommended.

Available local measurements of S_t can be used to carry out a regression analysis to determine the angstrom coefficients a_s and b_s by comparing with S_0 on overcast days to give a_s, and on days with bright sunshine to give $(a_s + b_s)$. Depending on atmospheric conditions (humidity, dust) and solar declination (latitude and month), the values of a_s and b_s will vary. When no actual solar radiation data are available, and no calibration has been carried out for improved a_s and b_s parameters, the following values are recommended for average climates:

$$a_s = 0.25 \qquad \text{and} \qquad b_s = 0.50$$

Net Long-Wave Radiation. There is a significant exchange of radiant energy between the earth's surface and the atmosphere in the form of radiation at longer wavelengths, i.e., in the range 3 to 100 μm (see Fig. 4.2.2). Both the ground and the atmosphere emit black-body radiation with a spectrum characteristic of their temperature. Since the surface is on average warmer than the atmosphere, there is usually a net loss of energy as thermal radiation from the ground.

The exchange of long-wave radiation L_n between vegetation and soil on the one hand, and atmosphere and clouds on the other, can be represented by the following radiation law:

$$L_n = L_i - L_o = -f\epsilon'\sigma(T + 273.2)^4 \qquad \text{MJ m}^{-2}\text{ day}^{-1} \tag{4.2.7}$$

where L_o = outgoing long-wave radiation (ground to atmosphere), MJ m^{-2} day^{-1}
L_i = incoming long-wave radiation (atmosphere to ground), MJ m^{-2} day^{-1}
f = adjustment for cloud cover
ϵ' = net emissivity between the atmosphere and the ground
σ = Stefan-Boltzmann constant (4.903×10^{-9} MJ m^{-2} °K^{-4} day^{-1})
T = mean air temperature, °C

The *net emissivity* ϵ' can be estimated[3,14] from

$$\epsilon' = a_e + b_e\sqrt{e_d} \tag{4.2.8}$$

where e_d = vapor pressure, kPa
a_e = correlation coefficient
b_e = correlation coefficient

a_e lies in the range 0.34 to 0.44 and b_e in the range -0.14 and -0.25, but for average conditions the following indicative values can be taken:[30]

$$a_e = 0.34 \qquad \text{and} \qquad b_e = -0.14$$

When humidity measurements are not available, the dew point at minimum temperature can be taken to estimate average vapor pressure. Alternatively net emissivity can be estimated[53] from average temperature (in degrees Celsius) according to the equation

$$\epsilon' = -0.02 + 0.261\exp(-7.77 \times 10^{-4}\,T^2) \tag{4.2.9}$$

The *cloudiness factor* f in Eq. (4.2.7) can be estimated[135] using solar radiation data from

$$f = a_c\frac{S_t}{S_{to}} + b_c \tag{4.2.10}$$

where S_t = measured solar radiation
S_{to} = solar radiation for clear skies [Eq. (4.2.6) with $n/N = 1$]
a_c, b_c = long-wave radiation coefficients for clear skies (sum = 1.0)

a_c and b_c parameters are calibration values to be determined through specialized local studies which involve measuring long-wave radiation values. The following indicative values are recommended:[30]

$$a_c = 1.35 \qquad b_c = -0.35 \qquad \text{(arid areas)}$$

$$a_c = 1.00 \qquad b_c = 0.00 \qquad \text{(humid areas)}$$

When data on sunshine hours n are available, the cloudiness factor for partly cloudy skies can be determined by substituting the relevant terms of Eq. (4.2.6) into Eq. (4.2.10) to give

$$f = \left(a_c \frac{b_s}{a_s + b_s}\right)\frac{n}{N} + \left(b_c + \frac{a_s}{a_s + b_s} a_c\right) \tag{4.2.11}$$

For $a_c = 1.35$, $b_c = -0.35$, $a_s = 0.25$, and $b_s = 0.50$, this becomes

$$f = 0.9\frac{n}{N} + 0.1 \tag{4.2.12}$$

Net Radiation. The *net radiation* R_n is the net input of radiation at the surface, i.e., the difference between the incoming and reflected solar radiation, plus the difference between the incoming long-wave radiation and outgoing long-wave radiation (see Fig. 4.2.2). It is given by

$$R_n = S_n + L_n \qquad \text{MJ m}^{-2}\text{ day}^{-1} \tag{4.2.13}$$

Net radiation is comparatively simple to measure using instrumentation, and indirect measurement is increasingly possible using satellite data,[91] albeit with considerable uncertainty. Often, however, practicing hydrologists are required to provide estimates of evaporation from data records which do not include net radiation. In these circumstances S_n must be estimated from Eqs. (4.2.5) and (4.2.6), and L_n from Eq. (4.2.7) and associated equations. Using the indicative values given in previous sections, for general purposes when only sunshine, temperature, and humidity data are available, net radiation (in MJ m^{-2} day^{-1}) can be estimated by the following equation: $(1-\alpha)$

$$R_n = \left(0.25 + 0.5\frac{n}{N}\right)S_0 - \left(0.9\frac{n}{N} + 0.1\right)(0.34 - 0.14\sqrt{e_d})\sigma T^4 \tag{4.2.14}$$

Because of the strong link between energy and evaporation (through the latent heat of vaporization; see Sec. 4.2.1), R_n can be expressed as an equivalent depth of evaporated water in mm by dividing R_n by $\rho_w \lambda$ where ρ_w (in kg m^{-3}) is the density of water, and λ is the latent heat of vaporization (in MJ kg^{-1}) from Eq. (4.2.1). It is convenient that with R_n in MJ m^{-2} day^{-1} the numerical value (R_n/λ) gives equivalent water depth in mm day^{-1}, since $\rho_w \approx 1000$ kg m^{-3}.

4.2.3 Energy Budget for a Unit Area

When describing the evaporation process it is usual to draw up an energy budget for a volume of defined vertical extent and unit area in the horizontal plane. In the case of

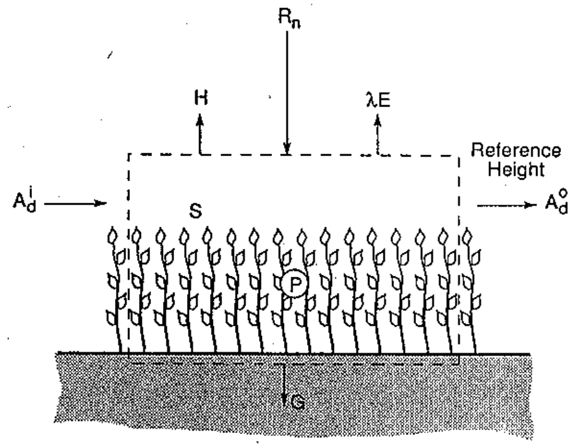

FIGURE 4.2.3 The components of the energy balance for a volume extending from just below the soil surface to the height at which the net radiation balance is determined.

a crop this volume extends from just below the soil surface, where energy lost by heat conduction to the soil is measured or estimated, to that level above the canopy at which the radiation balance described in the previous section is defined.

Figure 4.2.3 illustrates the components of the whole canopy energy balance for daytime conditions, which, ranked in approximate order of their magnitude, comprise:

R_n = net incoming radiant energy

λE = outgoing energy as evaporation

H = outgoing sensible heat flux

G = outgoing heat conduction into the soil

S = energy temporarily "stored" within the volume, and often neglected except for forests,[116] proportional to temperature changes in the vegetation, air, and shallow soil layer; and to changes in atmospheric humidity

P = energy absorbed by biochemical processes in the plants, typically taken as 2 percent of net radiation[116]

A_d = loss of energy associated with horizontal air movement;[119] significant in an "oasis" situation, but generally neglected otherwise ($A_d = A_d^o - A_d^i$ in Fig. 4.2.3)

It is usual to collect the energy terms and define an entity A, *the available energy*, which is the energy available for partitioning into latent or sensible heat. For the case of a complete canopy

and
$$A = \lambda E + H \tag{4.2.15}$$
$$A = R_n - G - S - P - A_d \qquad \text{MJ m}^{-2}\text{ day}^{-1} \tag{4.2.16}$$

Conduction is the main mechanism for heat transfer in soils. In the idealized case of a uniform soil, and assuming the temperature of the soil-air interface oscillates sinusoidally over a day or a year, the heat flow is maximized when the rate of change of the soil surface temperature is greatest, one-eighth of a cycle before the peak temperature, i.e., 3 h earlier in the case of the diurnal wave and 1½ months earlier in the case of the annual wave. The amplitude of the daily cycle in soil surface temperature can be significantly greater than that in air temperature, with timing mainly linked to radiation input, and soil heat conduction G can be large, typically 30 percent of the net radiation exchange at the soil surface. With dense vegetation, little radiation reaches the ground and heat storage in the soil can often be neglected.[109]

The effective soil depth to which heat is transferred is greater for longer temperature cycles. To estimate the change in soil heat content for a given period, the following equation can be used:[126]

$$G = c_s d_s \frac{T_2 - T_1}{\Delta t} \qquad \text{MJ m}^{-2}\text{ day}^{-1} \tag{4.2.17}$$

where T_2 = temperature at the end of the period, °C
T_1 = temperature at the beginning of the period, °C
Δt = length of period, days
c_s = soil heat capacity (2.1 MJ m^{-3} °C^{-1}) for average moist soil
d_s = estimated effective soil depth, m

For *daily* temperature fluctuations (effective soil depth typically 0.18 m) the above formula[136] becomes

$$G = 0.38\,(T_{\text{day}\,2} - T_{\text{day}\,1}) \qquad \text{MJ m}^{-2}\text{ day}^{-1} \tag{4.2.18}$$

For *monthly* temperature fluctuations (effective soil depth typically 2.0 m)[56] it becomes

$$G = 0.14\,(T_{\text{month}\,2} - T_{\text{month}\,1}) \qquad \text{MJ m}^{-2}\text{ month}^{-1} \tag{4.2.19}$$

Since the magnitude of daily soil heat flux over 10- to 30-day periods is relatively small, it can often be neglected in hydrologic applications.

Heat transfer to depth in a water body is by conduction and thermal convection, and by the penetration of radiation below the surface. Its calculation is complex, and it is easier to measure it from successive temperature profile surveys.[27] The sensible heat transferred into a lake by water inflow and outflow A_h may be significant in the energy budget of a whole lake. The total advection rate per unit lake area can be approximated as follows:

$$\left.\begin{aligned} A_h &= \rho_w c_w\,(q_i T_i - q_o T_o + P T_p) \\ &= 4.19 \times 10^{-3}\,(q_i T_i - q_o T_o + P T_p) \end{aligned}\right\} \qquad \text{MJ m}^{-2} \tag{4.2.20}$$

where ρ_w is the density of water, c_w is its specific heat; q_i and q_o are the rate of inflow and outflow per unit area of lake, P is the rate of precipitation (all in mm); and T_i, T_o, and T_p are the temperatures (in °C) of the inflow, outflow and precipitation water, respectively.

4.2.4 Diffusion through the Air

The extent to which the energy available at the ground is used to evaporate water is determined by the processes controlling vapor diffusion through the air. Movement

occurs where there are variations in vapor concentration, and because the molecules making up the air are in permanent, random motion, either individually or in coherent groups as turbulent eddies. Eddy circulation raises moist air from near the land surface and replaces it with drier air from higher up, resulting in a net upward moisture movement in proportion to the vapor concentration difference between the upper and lower air masses.

The flows of water vapor λE and sensible heat H are proportional to differences in the vapor pressure e and temperature T, respectively. The constant of proportionality is related to the transport *resistance*, which measures the restriction placed on the movement by the diffusion process.

Molecular Diffusion. Individual air molecules are in rapid, haphazard motion at normal temperatures. The transfers associated with such motion control the movement of water vapor and warmed air at or near the leaves and stems within vegetation, and near the surface of the underlying soil. Air moving within vegetation, for instance, can be envisaged as interacting with leaves through the boundary layer of slowly moving air which surrounds each leaf. The rate of vapor flow is controlled by a *boundary-layer resistance*.[24,57,119] Similarly, a simple representation of evaporation within soil might assume, for instance,[71] that water vapor moves by molecular diffusion in the air between the soil particles in a progressively deepening layer of dry soil, thus producing a *soil surface resistance*.[112]

However, the most important resistance associated with molecular diffusion is that which controls the movement of water vapor from inside plant leaves to the air outside through small apertures in the surface of the leaves which are called *stomata*. Figure 4.2.4 illustrates this *transpiration* process. The air inside the stomatal cavity beneath the leaf surface is nearly saturated, while that outside is usually less. Water vapor movement is controlled by the plant, which opens or closes the stomatal aperture in response to atmospheric moisture demand and the amount of water in the soil. In this way, plants control their water loss to the atmosphere, and seek to ensure their survival when water is limited.

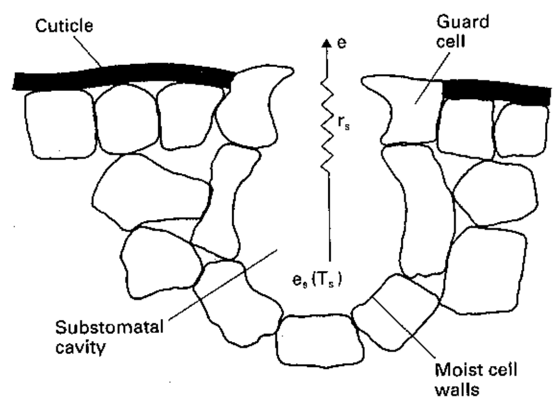

FIGURE 4.2.4 Transpiration by molecular diffusion of water vapor through the stomatal aperture of dry leaves. Air inside the substomatal cavity is saturated at the temperature of the leaf, and the water vapor diffuses through the stomatal opening to the less saturated atmosphere against a stomatal resistance which, for the whole canopy, is called the surface resistance r_s.

The stomatal resistance of the whole canopy, referred to as the *surface resistance* r_s, is less when more leaves are present since there are then more stomata through which transpired water vapor can diffuse. Empirical relationships exist between the surface resistance and leaf cover, soil water status, and environmental variables (e.g., Ref. 106) which can provide relationships suitable for practical application in estimating evaporation.

An analogy may be drawn with electrical resistance. The current i through a wire of resistance R is related to the potential difference V between the ends of the wire by Ohm's law, $V = iR$, which may be rewritten for the current i as $i = V/R$. Now in vapor transport, the measure of potential is the vapor pressure and the equivalent of current is the vapor flux rate E. Thus the vapor flux rate can be approximately estimated for leaf stomata as

$$E = \frac{k(e_s - e)}{r_s} \qquad (4.2.21)$$

where k is a constant to account for units. The dimensions of vapor flow resistance r_s are $(T\,L^{-1})$ usually measured in s m^{-1}.

One approximation[2] for r_s is

$$r_s = \frac{200}{L} \quad \text{s m}^{-1} \qquad (4.2.22)$$

If h_c is the mean height of the crop, then the leaf area index L can be estimated[3] by

$$L = 24\,h_c \quad \text{(clipped grass with } 0.05 < h_c < 0.15 \text{ m)}$$
$$L = 5.5 + 1.5 \ln(h_c) \quad \text{(alfalfa with } 0.10 < h_c < 0.50 \text{ m)} \qquad (4.2.23)$$

The *surface resistance of the reference crop* of clipped grass 0.12 m high (see Sec. 4.1.1) is estimated as

$$r_s^{rc} = 69 \quad \text{s m}^{-1} \qquad (4.2.24)$$

Turbulent Diffusion. The wind blowing horizontally over natural surfaces is retarded by interaction with the ground and vegetation. This interaction creates random and haphazard air motion in which portions of air, of varying size, move in an ill-defined yet coherent way during their transient existence. This phenomenon, known as *turbulence*, is a much more efficient transport mechanism than molecular diffusion and is the primary process responsible for exchange between air close to the ground and that at higher levels in the atmosphere.

The rate of water vapor transfer away from the ground by turbulent diffusion is controlled by *aerodynamic resistance* r_a, which is inversely proportional to wind speed and changes with the height of the vegetation covering the ground, as

$$r_a = \frac{\ln[(z_u - d)/z_{om}]\ln[(z_e - d)/z_{ov}]}{(0.41)^2\,U_z} \quad \text{s m}^{-1} \qquad (4.2.25)$$

where z_u and z_e are the respective heights of the wind speed and humidity measurements, and U_z is the wind speed. Estimates can be made of r_a by assuming[15] that $z_{om} = 0.123\,h_c$ and $z_{ov} = 0.0123\,h_c$, and[71] that $d = 0.67\,h_c$, where h_c is the mean height of the crop.

If wind speed and humidity measurements are made at a height of (say) 2 m above

the top of the vegetation, then for a measured wind speed of 5 m s^{-1}, Eq. (4.2.25) gives values of 45 s m^{-1}, 18 s m^{-1}, and 6.5 s m^{-1} for the aerodynamic resistance for grass ($h_c = 0.1$ m), agricultural crops ($h_c = 1.0$ m), and forest ($h_c = 10$ m), respectively. The rate of diffusion of water vapor is greater where the resistance to vapor diffusion is less, so the aerodynamic exchange of taller crops is more efficient than for shorter crops. In consequence, water caught on their leaves during rainstorms or overhead irrigation evaporates more quickly from taller crops as compared to shorter crops.

The *aerodynamic resistance of the reference crop* (see Sec. 4.1.1) with a crop height of 0.12 m, and for measurements of temperature and humidity at a standardized height of 2.0 m, is given by

$$r_a^{rc} = \frac{208}{U_2} \quad \text{s m}^{-1} \qquad (4.2.26)$$

where U_2 is the wind speed in m s^{-1}, also measured at 2 m.

4.2.5 Simulation by Resistance Networks

In advanced models of evaporation, the diffusion of energy in the form of sensible heat or water vapor away from the plants or soil into the atmosphere is represented by a network of resistances of the types described in the previous section. Such models can be complex, with the plant canopy broken into separate layers and evaporation rates calculated from each of these individually.[113,126–128]

It is also possible to build physically realistic descriptions of sparse canopies using equivalent resistance networks which consider the evaporation from the plants separately to that from the soil.[45,61,111,112] Such models do not yet, however, have widespread use among practicing hydrologists.

Penman-Monteith Equation. Currently the most advanced resistance-based model of evaporation used in hydrologic practice assumes that all the energy available for evaporation is accessible by the plant canopy, and water vapor diffuses first out of the leaves against the surface (or stomatal) resistance r_s and then out into the atmosphere above against the aerodynamic resistance. Meanwhile the sensible heat, which originates outside rather than inside the leaves, only has to diffuse upward against the aerodynamic resistance r_a. This model is represented diagrammatically in Fig. 4.2.5.

Solving the equations describing the diffusion processes represented in Fig. 4.2.5 produces the Penman-Monteith equation. This equation allows the calculation of evaporation from meteorological variables and resistances which are related to the stomatal and aerodynamic characteristics of the crop, and has the form[72]

$$E = \frac{1}{\lambda}\left[\frac{\Delta A + \rho_a c_p D/r_a}{\Delta + \gamma(1 + r_s/r_a)}\right] \quad \text{mm day}^{-1} \qquad (4.2.27)$$

in which Δ is given by Eq. (4.2.3), A by Eq. (4.2.16); D is the vapor pressure deficit $(e_s - e)$ (in kPa) measured at the height z_e for which r_a is calculated from Eq. (4.2.25); and r_s is the surface resistance of the land cover. The *psychrometric constant* γ is defined by the equation

$$\gamma = \frac{c_p P}{\epsilon\lambda} \times 10^{-3} = 0.0016286\,\frac{P}{\lambda} \quad \text{kPa °C}^{-1} \qquad (4.2.28)$$

where c_p is the specific heat of moist air ($= 1.013$ kJ kg^{-1} °C^{-1}), P is the atmospheric

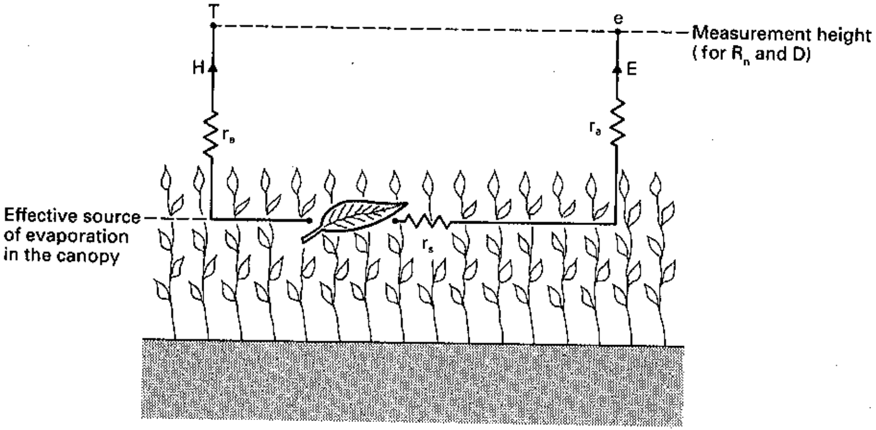

FIGURE 4.2.5 The equivalent network of diffusion resistances representing evaporation from an established crop canopy which intercepts almost all of the sun's radiant energy. It is assumed to share the available energy A as evaporation E or sensible heat H in the same way as would a single equivalent "big leaf" positioned at the effective source height $(d + z_o)$ within the crop.

pressure (in kPa), ϵ is the ratio of the molecular weight of water vapor to that for dry air ($=0.622$), and λ is the latent heat of vaporization of water (MJ kg^{-1}) given by Eq. (4.2.1). Values of γ as a function of air temperature are given in Table 4.2.1.

Wet Canopies. When vegetation is wet, which might be the case during or immediately after rain or following sprinkler irrigation, the source of water vapor is no longer inside the leaves; rather it is the water on the plants' surface. The stomata are no longer effective in restricting evaporation, and the surface resistance $r_s = 0$. For short crops, such as grass, r_a is large (see Sec. 4.2.4) and the consequence of setting $r_s = 0$ in Eq. (4.2.27) is less for grass than it is for tall vegetation such as forest.

The enhanced rate of evaporation of the water intercepted by forest during rain is an important aspect of the hydrologic effects of land-use change involving afforestation or deforestation (see Chap. 13). To make realistic estimates of forest evaporation it is necessary to describe the transpiration and the evaporation of rainwater separately. The latter component, the rainfall interception loss, can be estimated using models which calculate a running water balance for the storm water stored on the vegetation (e.g., Refs. 98, 99) from frequently sampled measurements of meteorological variables, including hourly rainfall.

Potential Evaporation Equation. Since potential evaporation occurs from an extensive free water surface, it follows that $r_s = 0$ is the appropriate value of surface resistance for estimating potential evaporation from Eq. (4.2.27). Further, the relevant value of energy supply A is given by replacing the smaller terms in Eq. (4.2.16) by A_h in Eq. (4.2.20), so that $A = (R_n + A_h)$. The appropriate form of r_a for open water evaporation was first determined empirically,[80,81] but its physical basis is now better understood,[121] and it can be estimated from

$$r_a^p = \frac{4.72\,[\ln (z_m/z_o)]^2}{1 + 0.536\,U_2} \quad \text{s m}^{-1} \tag{4.2.29}$$

where z_m (in m) is the height at which meteorological variables are measured, and z_o (in m) is the aerodynamic roughness of the surface.

For a standardized measurement height for wind speed, temperature, and humidity measurements of 2 m, and adopting the value $z_0 = 0.00137$ m which, according to Thom and Oliver[121] is that implicitly assumed by Penman,[80,81] *the equation here recommended for estimating potential evaporation E_p* (in mm day^{-1}) *is*

$$E_p = \frac{\Delta}{\Delta + \gamma}(R_n + A_h) + \frac{\gamma}{\Delta + \gamma}\,\frac{6.43\,(1 + 0.536\,U_2)D}{\lambda} \tag{4.2.30}$$

where R_n = net radiation exchange for the free water surface, mm day^{-1}
A_h = energy advected to the water body, mm day^{-1}, if significant
U_2 = wind speed measured at 2 m, m s^{-1}
D = vapor pressure deficit $e_s - e$, kPa

and λ, Δ, and γ are given by Eqs. (4.2.1), (4.2.3), and (4.2.28), respectively.

Reference Crop Evaporation Equation. In this chapter the reference crop is precisely defined in terms of parameters appropriate to Eq. (4.2.27); see Sec. 4.1.1. Combining Eqs. (4.2.4), (4.2.16), (4.2.24), (4.2.27), and (4.2.28) [but neglecting the minor terms in Eq. (4.2.16)], and for a standardized measurement height for wind speed, temperature, and humidity of 2 m, *the equation here recommended for estimating reference crop evaporation,* in mm day^{-1}, *is*

$$E_{rc} = \frac{\Delta}{\Delta + \gamma^*}(R_n - G) + \frac{\gamma}{\Delta + \gamma^*}\,\frac{900}{T + 275}\,U_2\,D \tag{4.2.31}$$

where R_n = net radiation exchange for the crop cover, mm day^{-1}
G = measured or estimated soil heat flux, mm day^{-1}
T = temperature, °C
U_2 = wind speed at 2 m, m s^{-1}
D = vapor pressure deficit, kPa

and

$$\gamma^* = \gamma(1 + 0.33\,U_2) \tag{4.2.32}$$

It should be noted that Eq. (4.2.31) is *not the Penman-Monteith equation as such,* since this equation has broader applicability. Rather Eqs. (4.2.30) and (4.2.31) are both implementations of the Penman-Monteith equation, in which the several resistances are here assigned particular values for specific, well-defined reference surfaces.

4.2.6 Empirical Estimation Equations

The physically-based equations for estimating evaporation rates for open water and reference crops recommended in the previous section, which are based on equivalent resistance networks, are currently the most physically realistic equations available for hydrologic application. Historically, conceptually simpler equations have been proposed, which are less fundamental and therefore necessarily have greater empirical content. Viewed in retrospect, these can be considered as simplifications of Eqs. (4.2.30) and (4.2.31) through the introduction of empirical relationships between meteorological variables derived from local data.

All the equations given below provide estimates of evaporation for a reference crop, and this is their primary purpose. In general they can also be considered to provide an approximate estimate of the potential evaporation rate for open water surfaces. However, in this case those equations which explicitly contain the available energy appropriate to a reference crop, i.e., $(R_n - G)$, should have this replaced by $(R_n + A_h)$, this being the equivalent form appropriate to a free water surface [see Eqs. (4.2.30) and (4.2.31)].

Combination Equations. Penman[80] was the first to derive an equation, given earlier as Eq. (4.2.30), which combines the energy required to sustain evaporation and an empirical description of the diffusion mechanism by which energy is removed from the surface as water vapor. Because it combines energy and diffusion features, this equation became known as a *combination equation,* and it spawned sibling equations which are given by "tuning" the empiricism in the description of atmospheric diffusion to better represent particular sets of data or local conditions, e.g., Refs. 30, 82, and 135.

When analyzing the link between the Penman and the Penman-Monteith equations, Thom and Oliver[121] demonstrated that Penman's implicit empirical function for the aerodynamic resistance [see Eq. (4.2.29)] not only provides some allowance for the effect of atmospheric buoyancy but also, when applied to a reference crop, makes approximate allowance for the absence of a surface resistance in the denominator, comparing Eqs. (4.2.27) and (4.2.30).

Studies of the comparative performance of several different forms of the combination equation[56] suggest that "tuning" the representation of the diffusion component has little universal advantage, though the introduction of some empirical seasonal dependence may be beneficial. This conclusion is consistent with Thom and Oliver's interpretation. The seasonal adjustment currently favored is based on data from Kimberly, Idaho, and the resulting Kimberly Penman equation[56,134] has the same nomenclature as Eq. (4.2.30) and takes the form

$$E_{rc} = \frac{\Delta}{\Delta + \gamma}(R_n - G) + \frac{\gamma}{\Delta + \gamma}\frac{6.43\ W_f D}{\lambda} \qquad \text{mm day}^{-1} \tag{4.2.33}$$

where

$$W_f = a_w + b_w U_2 \tag{4.2.34}$$

$$a_w = 0.4 + 1.4 \exp\{-[(J - 173)/58]^2\} \tag{4.2.35}$$

in which J is the Julian day number with, for northern latitudes,

$$b_w = 0.605 + 0.345 \exp\{-[(J - 243)/80]^2\} \tag{4.2.36}$$

and, for southern latitudes, J set to $J' = (J - 182)$ for $J \gtrsim 182$, and set to $J' = (J + 183)$ for $J < 182$.

Radiation-Based Equations. The first term in Eq. (4.2.33) frequently exceeds the second term by a factor of about 4, and this suggests the possibility of a simpler empirical relation between reference crop evaporation rate and radiation called the Priestley-Taylor equation with the general form[86]

$$E_{rc} = \alpha \frac{\Delta}{\Delta + \gamma}(R_n - G) \qquad \text{mm day}^{-1} \tag{4.2.37}$$

In fact there is now more substantial evidence supporting such an empirical relationship, at least on a regional average (as opposed to a crop-specific) basis, for regions with uniform vegetation cover, or with land cover which is heterogeneous at the scale of a few kilometers.[104,107] Simple models of the evaluation of the near-surface atmospheric boundary layer[13,67,68] overviewed in Sec. 4.2.7 suggest that its partial containment by a thermal inversion layer in the atmosphere yields near surface vapor pressures in the second term of Eq. (4.2.33) which support a value of $\alpha \approx 1.26$ in Eq. (4.2.37) for $r_s = 69$ s m^{-1}.

Recent evaluation[56] of Eq. (4.2.37) with $\alpha = 1.26$ confirms its applicability in humid climates. However, in arid climates the value of $\alpha = 1.74$ provides better estimates (Ref. 56, Table 7.16). On the basis of these results, and in view of its inherent simplicity, *the radiation-based equations here recommended for reference crop evaporation estimation are*

$$E_{rc} = 1.74 \frac{\Delta}{\Delta + \gamma}(R_n - G) \qquad \text{mm day}^{-1} \tag{4.2.38}$$

for arid locations, with relative humidity less than 60 percent in the month having peak evaporation, and

$$E_{rc} = 1.26 \frac{\Delta}{\Delta + \gamma}(R_n - G) \qquad \text{mm day}^{-1} \tag{4.2.39}$$

at all other (humid) locations.

Certain other empirical radiation-based equations remain in common use. *In humid climates,* the Turc equations[125] have been shown[52] to perform well. These equations have the form for RH < 50 percent

$$E = 0.31 \frac{T}{T + 15}(S_n + 2.09)\left(1 + \frac{50 - \text{RH}}{70}\right) \qquad \text{mm day}^{-1} \tag{4.2.40}$$

and for RH > 50 percent

$$E = 0.31 \frac{T}{T + 15}(S_n + 2.09) \qquad \text{mm day}^{-1} \tag{4.2.41}$$

where T is the average temperature in °C, S_n is the water equivalent of net solar radiation in mm day^{-1}, and RH is the relative humidity in percent. The general similarity in form between these earlier equations and Eqs. (4.2.38) and (4.2.39) is to be expected.

In arid climates, on the other hand, the radiation-based equation of Doorenbos and Pruitt,[30] which takes the form

$$E = -0.3 + b_{dp} \frac{\Delta}{\Delta + \gamma} S_n \qquad \text{mm day}^{-1} \tag{4.2.42}$$

has been shown[56] to provide estimates of reference crop evaporation, with[35]

$$b_{dp} = 1.066 - 0.0013\,(\text{RH}_{\text{mean}}) + 0.045\,(U_d) - 0.0002\,(\text{RH}_{\text{mean}})\,(U_d) - 0.000315\,(\text{RH}_{\text{mean}})^2 - 0.0011\,(U_d)^2 \tag{4.2.43}$$

where RH_{mean} is mean relative humidity in percentage, U_d is the mean daytime wind speed in m s^{-1}, and S_n is the net solar radiation in mm day^{-1}; see Eq. (4.2.5).

Temperature-Based Equations. The physical basis for estimating evaporation using temperature alone is that both terms in Eq. (4.2.31) are likely to have some relationship with temperature. Since the first (radiation-dependent) term is generally much the larger of the two, it is the correlation between radiation and temperature which is most important. The yearly temperature cycle is delayed with respect to the yearly radiation cycle and the empiricism in some past formulas has included allowance for this thermal lag.

In general, the only justification for using estimation equations of this type is that prediction of evaporation is required on the basis of existing data in which temperature is the only available variable measurement, and even in this case it is unwise to make evaporation estimates for less than a monthly averaging period. Certain relationships merit mention either because their relationship to radiation-based estimates is more explicit and plausible or because their empiricism is very broadly based and they are in very common use. Only the Hargreaves equation and Blaney-Criddle method are described below. Other temperature-based methods are not recommended.

The Hargreaves equation[47–50] is here taken as

$$E_{rc} = 0.0023\, S_o\, \bar{\delta}_T\, (T + 17.8) \qquad \text{mm day}^{-1} \tag{4.2.44}$$

where S_o is the water equivalent of extraterrestrial radiation in mm day^{-1} for the location of interest [see Eq. (4.4.4)], T is the temperature in °C, and $\bar{\delta}_T$ is the difference between mean monthly maximum and mean monthly minimum temperatures. This equation has been shown[56] to provide at least reasonable estimates of reference crop evaporation. Presumably this is because it contains an explicit link to solar radiation through S_o; some measure of the extent to which this radiation reaches the surface and warms the air near the ground, through the factor $\bar{\delta}_T$; while the temperature variation in $(T + 17.8)$ approximates the value of $\Delta/(\Delta + \gamma)$.

The Blaney-Criddle method[11,30] is well known and still in common use, and it is included here for this reason alone. In its most modern complex form[4,30,35] it contains much empiricism, and it is now hard to consider it merely a temperature-based method. The currently preferred form of the equation is

$$E = a_{BC} + b_{BC} f \tag{4.2.45}$$

with

$$f = p\,(0.46T + 8.13) \tag{4.2.45a}$$

$$a_{BC} = 0.0043\ \mathrm{RH}_{\min} - (n/N) - 1.41 \tag{4.2.45b}$$

$$b_{BC} = 0.82 - 0.0041\,(\mathrm{RH}_{\min}) + 1.07\,(n/N) + 0.066\,(U_d) - 0.006\,(\mathrm{RH}_{\min})\,(n/N) - 0.0006\,(\mathrm{RH}_{\min})\,(U_d) \tag{4.2.45c}$$

where p is the ratio of actual daily daytime hours to annual mean daily daytime hours expressed as a percent, T is mean air temperature in °C, (n/N) is the ratio of actual to possible sunshine hours, $\mathrm{RH}_{\min}$ is the minimum daily relative humidity in percentage, and U_d is the daytime wind at 2 m height in m s^{-1}. The complexity of this equation is a tribute to the loyalty of its proponents, but precludes its ready interpretation in terms of a physically realistic equivalent.

4.2.7 Atmospheric Feedbacks

Changes in surface energy exchange alter the air as the atmosphere passes over variable land cover. Initially this change is immediately adjacent to the surface; then it moves progressively upward through the near-surface turbulent layer, finally permeating the whole planetary boundary layer and then the atmosphere above. In so doing, those properties of the air which control surface evaporation rate can be altered, and a feedback may occur to moderate the influence of changes in surface cover. This modification of the atmosphere happens at all horizontal scales, from the very small scale of the leaf or an evaporation pan, through the intermediate scale of the lake or irrigated field, and then at the regional and even continental scale.

Evaporation from Small Areas (Oasis Effect). Empirical and theoretical studies have been made of the evaporation from uniformly moist surfaces of limited extent, such as evaporation pans or lakes (e.g., Refs. 18, 19, 20, and 46) or moist grass[90] surrounded by dry ground. Although the effect of a change in surface cover propagates upward into the atmosphere fairly slowly, studies with numerical models of atmospheric turbulence suggest that the adjustment of the surface evaporation rate into a moving airstream as the air passes on to a different type of evaporative surface occurs quickly, within (say) 5 to 10 m of the boundary between the two surfaces (see Fig. 4.2.6).

In the case of water bodies the area of the water surface changes the effective size of the aerodynamic resistance (see Sec. 4.2.4) between the surface of the water, where the vapor pressure is e_{sf}, and the standardized height of 2 m at which the average vapor pressure and wind speed are e and U_2, respectively. The evaporation rates (in mm day^{-1}) for a water surface of area A (in m^2) are adequately described in Ref. 16 for pans, with $0.5\ \text{m} < A^{0.5} < 5$ m, by

$$E = 3.623\, A^{-0.066}\, (e_{sf} - e)\, U_2 \tag{4.2.46}$$

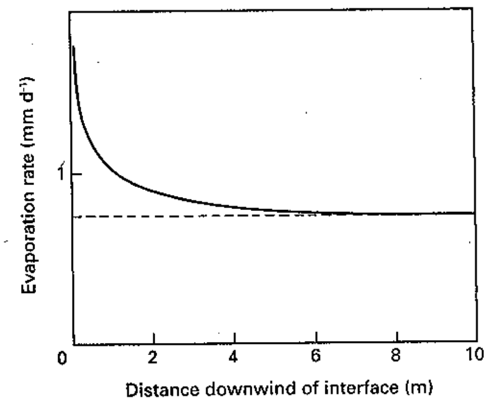

FIGURE 4.2.6 Predicted change in *surface* evaporation rate downwind of an interface between a dry, smooth surface and a well-watered, grassy area (reference crop) on a sunny day. *(Redrawn from Rao et al.[90] Used with permission.)*

and for lakes, with 50 m $< A^{0.5} <$ 100 km, by

$$E = 2.909\, A^{-0.05}\, (e_{sf} - e)\, U_2 \qquad (4.2.47)$$

in which e and e_{sf} are in kPa, and e_{sf} can be assumed to be the saturated vapor pressure corresponding to the surface temperature of the water [see Eq. (4.2.2)].

Regional Scale Evaporation. There has long been an intuitive belief among hydrologists that atmospheric feedback mechanisms intervene at the regional scale to moderate the effect of surface controls on evaporation. It is the basis of the hypothetical potential evaporation rates defined in Sec. 4.1.1.

Faith in the concept of potential evaporation rates grew so strong that Bouchet[12] and Morton[73–76] postulated that the equilibrium around the hypothetical, potential evaporation λE_{po} which *would* have been applicable had water been freely available might provide a means of estimating actual evaporation. They postulate that the *excess* potential demand above this "preferred" potential rate as calculated from estimates of the potential evaporation λE_o using near-surface weather variables is directly related to the "short fall" in the actual evaporation λE due to restricted water availability, that is,

$$\lambda E_{po} - \lambda E = \lambda E_o - \lambda E_{po} \qquad (4.2.48)$$

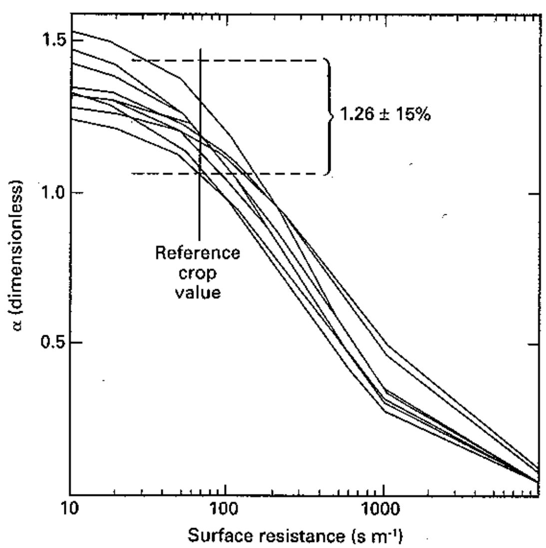

FIGURE 4.2.7 The effective daytime average value of the Priestley-Taylor parameter α in Eq. (4.2.37) as synthesized from a simple one-dimensional planetary boundary layer model. *(From McNaughton and Spriggs.[68] Used with permission.)* The several different lines correspond to model initializations with different radiosonde ascents drawn from data collected in the Netherlands.[31] Also shown is the value of surface resistance for a reference crop, and the preferred value of $\alpha = 1.26$ for humid climates [see Eq. (4.2.39)] with the range ±15 percent around this value.

Brutsaert and Stricker[17] had some success with this concept by substituting E_p calculated from Eq. (4.2.30) for λE_{po}, and λE_{rc} from Eq. (4.2.39) for λE_o, but recent modeling studies[68] have raised doubt about the hypothesis.

Over extensive uniform surfaces, or where surface changes occur at a small scale and in a haphazard way so that mixing of the air makes them appear uniform to the atmosphere, regional scale atmospheric feedback processes can be adequately represented by one-dimensional models. Such models[13,67,68] have provided better though still incomplete understanding, with broad support for a regional evaporation rate, though they highlight that the concept of a potential rate is only approximate and that it has significant dependency on the control exerted by vegetation and soil.

Currently, such modeling is limited to simulating the development of a one-dimensional atmospheric boundary in daylight conditions, with field data from radiosonde ascents[31] used to initiate the models and define the meteorological variables aloft. There is therefore no simulation of clouds or precipitation in these models. Nonetheless such models suggest that both the Penman equation [Eq. (4.2.30)] and the Priestley-Taylor equation [Eq. (4.2.39)] can provide reasonable simulation of *daytime* surface evaporation, and that the value $\alpha = 1.26$ in this last equation is acceptable to an accuracy of 15 percent for a range of area-average surface resistance typical of pasture and agricultural crops, including the reference crop ($r_s = 69$ s m^{-1}; see Sec. 4.1.1). Figure 4.2.7 shows the simulated variation in the preferred daytime average Priestley-Taylor parameter α as a function of the area-average surface resistance. The Bouchet[12] "complementary evaporation" hypothesis is not, however, supported[68] by these studies.

4.3 MEASUREMENT OF EVAPORATION

Natural evaporation can be measured either as the rate of loss of liquid water from the surface or as the rate of gain of water vapor by the atmosphere. Measurements in the liquid phase either assume or create a closed system, such as an evaporation pan or lysimeter, and deduce evaporation as the net loss of water from that closed system over a given time, the measurement being one of *discrete changes* in total quantity of water in the system. Measurements in the vapor phase most commonly assume that the atmosphere is an open system and determine evaporation as an integration of the *rate of flow* of water vapor (or equivalently latent heat) into that open system through the turbulent boundary layer near the land surface. Measurements of the net change in the vapor content of the air over large areas using balloons can provide estimates of regional evaporation rate,[66,79,92,114] but this approach does not yet form part of hydrologic practice. Most of the techniques described below provide measurements of the local evaporation rate, with the exception of catchment water balances which estimate area-average evaporation for confined watersheds.

4.3.1 Measurement of Liquid Water Loss

Measurements of this type draw up a mass or volume balance for the water in a specified volume of soil or in a body of liquid water. The surface area of this sample is a necessary part of the measurement, while its depth can either be well defined, as in lysimetric measurements, or poorly defined but large enough for vertical drainage to be either neglected or computed, as in watershed experiments. This difference influences the time scale over which the results are applicable. In each case the measurement reduces to determining the terms in a basic water balance equation which is applied over a particular time interval.

$$E = P - (V_R + V_S + V_L)/A \quad \text{mm} \tag{4.3.1}$$

where E = net evapotranspiration loss from the specified volume per unit area, mm
P = net precipitation (or irrigation) input to the specified volume per unit area, mm
V_R = net volume of liquid water entering or leaving the specified volume as measured inflow or outflow both above and below the surface, liters
V_S = change in liquid water stored within the specified volume, liters
V_L = "leakage," i.e., that total volume of liquid water leaving the specified volume which is not, or cannot be, measured, and which therefore represents an error in the method, liters
A = effective area of the sample volume at the land surface, m^2

All water budget measurements share the problem that the error in the evaporation calculated from Eq. (4.3.1) is an accumulation of the errors in the other measured variables.

Evaporation Pans. Because of its apparent simplicity, the evaporation pan is probably the instrument used most widely to estimate *potential* evaporation. However, Gangopadhyaya et al.[37] list 27 different designs of evaporation pans and suggest that their list "is undoubtedly far from complete."

Sunken pans (e.g., Colorado, USSR-GGI, USDA-BPI) are sometimes preferred in crop water requirement studies, since these pans have a water level at soil height and give a better direct prediction of reference crop evaporation than other pan designs.[88] The Colorado pan is 0.92 m square and 0.46 m deep. It is made of galvanized iron, set in the ground with the rim 0.05 m above ground level. The water level inside the pan is maintained at or slightly below ground level.

The U.S. Weather Bureau Class A pan is shown in Fig. 4.3.1. It is circular, 1.21 m in diameter and 0.255 m deep, and is made of galvanized iron (22 gauge) or monel metal (0.8 mm). The pan is mounted on a wooden open-frame platform with its bottom 0.15 m above ground level. The soil is built up to within 0.05 m of the bottom of the pan. The pan must be level. It is filled with water to 0.05 m below the rim, and the water level should not drop to more than 0.075 m below the rim. In semiarid countries it is quite common to cover the exposed water surface with mesh to stop animals from drinking the water. This lowers the evaporation measurement by 10 to 20 percent,[28] depending on the dimensions of the mesh.

The evaporation from a pan can differ significantly from that from an adjacent lake or surrounding vegetation. It is necessary to accommodate these sometimes large differences using empirical *pan coefficients*. Evaporation from pans is generally greater than from adjacent large areas of water or well-watered vegetation, but pan coefficients vary significantly with siting and pan design as well as with climatic factors.

Since pan data are widely available and much used for estimating crop water use for irrigation purposes, empirical pan coefficients have been derived, particularly for the U.S. Class A pan. Table 4.3.1 gives suggested values[30] for k^A_{pan} in the equation

$$E_{rc} = k^A_{\text{pan}} E^A_{\text{pan}} \qquad \text{mm day}^{-1} \tag{4.3.2}$$

for a range of conditions, and for pans sited in cropped fields (case A) and non-cropped, dry-surface fields (case B). In Eq. (4.3.2), E_{rc} is reference crop evaporation and E^A_{pan} is the measured Class A pan evaporation.

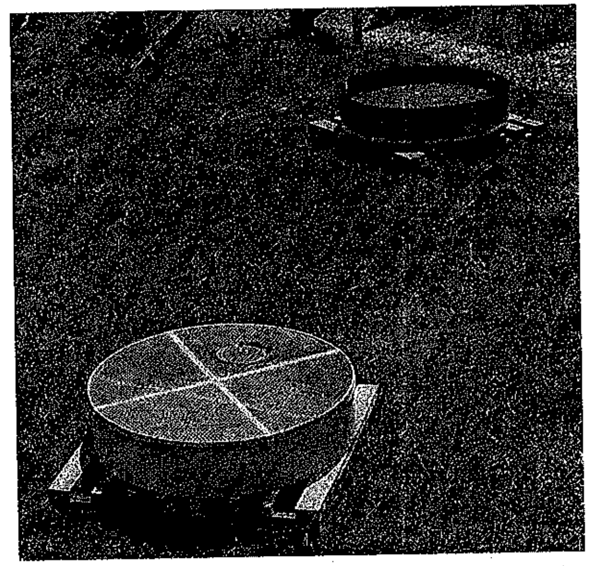

FIGURE 4.3.1 U.S. Weather Bureau Class A evaporation pans with screen in the foreground, and without screen in the background.

The wide range of coefficients given in Table 4.3.1 tends to overemphasize the shortcomings of pan data,[56] since most areas only occasionally experience the dry, strong wind conditions which give small k^A_{pan} values. Mean monthly E estimates based on pan evaporation should be within ±10 percent in most climates.

Water Balances of Watersheds and Lakes. River runoff is arguably the most accurate hydrologic measurement and is a valuable, direct determination of the available surface water resource. Careful gauging can provide stream-flow measurements accurate to about 2 percent. But considerable difficulties are involved in using the measured runoff from closed catchments to provide a worthwhile, indirect measurement of evaporation.[26,59,62,83,84,96,130,131] This is exacerbated in the case of lakes by the additional need to gauge inflow as well as outflow, and by enhanced difficulties in estimating subsurface seepage. Notwithstanding the above, carefully selected and well-managed paired watersheds can provide valuable and convincing evidence of the consequences of land-use change on evaporation (e.g., Ref. 59); see Chap. 13.

Accurate estimates of area average precipitation [P in Eq. (4.3.1)] are problematic,[132] not just because of the real likelihood of systematic gauging errors (e.g., Ref. 97) but also because of spatial variability associated with topographic and surface features for watersheds, and the need to estimate P from lakeside gauges in the case of precipitation over water bodies. Errors in estimating P, typically 5 to 10 percent, can increase markedly if a proportion of the precipitation falls as snow.

A systematic uncertainty in the evaporation loss deduced from a catchment water balance arises from the possibility that the unmeasured leakage V_L forms a significant part of the total water balance. Considerable skill is required in selecting natural catchments without leakage, and it is important to recognize that the subterranean groundwater contours play an important, perhaps definitive, role in specifying catchment boundaries and that surface topography is not necessarily a reliable reflection of subsurface flow direction.

TABLE 4.3.1 Suggested Values for the Pan Coefficient k_{pan}^A, Which Relates Reference Crop Evaporation E_{rc} to Measured Class A Pan Evaporation E_{pan}^A

Wind	Upwind fetch of green crop, m	Case A: Pan surrounded by short green crop — Mean relative humidity, %			Upwind fetch of dry fallow, m	Case B: Pan surrounded by dry, bare area — Mean relative humidity, %		
		Low <40	Med 40–70	High >70		Low <40	Med 40–70	High >70
Light (<1 m/s)	0	0.55	0.65	0.75	0	0.7	0.8	0.85
	10	0.65	0.75	0.85	10	0.6	0.7	0.8
	100	0.7	0.8	0.85	100	0.55	0.65	0.75
	1000	0.75	0.85	0.85	1000	0.5	0.6	0.7
Moderate (2–5 m/s)	0	0.5	0.6	0.65	0	0.65	0.75	0.8
	10	0.6	0.7	0.75	10	0.55	0.65	0.7
	100	0.65	0.75	0.8	100	0.5	0.6	0.65
	1000	0.7	0.8	0.8	1000	0.45	0.55	0.6
Strong (5–8 m/s)	0	0.45	0.5	0.6	0	0.6	0.65	0.7
	10	0.55	0.6	0.65	10	0.5	0.55	0.65
	100	0.6	0.65	0.7	100	0.45	0.5	0.6
	1000	0.65	0.7	0.75	1000	0.4	0.45	0.55
Very strong (>8 m/s)	0	0.4	0.45	0.5	0	0.5	0.6	0.65
	10	0.45	0.55	0.6	10	0.45	0.5	0.55
	100	0.5	0.6	0.65	100	0.4	0.45	0.5
	1000	0.55	0.6	0.65	1000	0.35	0.4	0.45

Source: After Doorenbos and Pruitt (Ref. 30). Used with permission.
Notes: Mean relative humidity is the average maximum and minimum daily relative humidities.
Case A: For pans surrounded by cropped fields or wet soils, with very dry soil beyond the prescribed fetch.
Case B: For pans surrounded by very dry soil, with cropped fields or wet soil beyond the prescribed fetch.

The change in storage term V_S in Eq. (4.3.1) is difficult to measure reliably in extensive natural catchments and will usually provide the most important error in a weekly or monthly evaporation measurement. Its significance becomes less for an annual determination, when the error from this component can become comparable with those in precipitation and runoff.

In the light of the very real possibility of significant error in the bulk evaporation loss deduced from a watershed, it is advisable to supplement any such derivations of evaporation with parallel and independent meteorological or lysimetric measurements.

Soil Moisture Depletion. Given sufficient measurements of soil moisture content to account for spatial variability in water storage, and provided that drainage is insignificant or can be quantified, measurements of change in V_S in Eq. (4.3.1) allow evaporation to be calculated when precipitation is either absent or separately determined. The technique requires the repeated, in situ measurement of soil water content, which is now possible with neutron probes, capacitance sounders, or time-domain reflectometers.[7–9,29,43,123,124]

When applying this method and these instruments, considerable care is required to avoid disturbing the plant canopy or altering the density, aeration, and infiltration characteristics of the soil surface.[87] Drainage losses from the soil sample can be significant.[58,77,95,117] When subterranean water movement occurs via unsaturated flow, frequent simultaneous measurement of soil water tension profiles[8] can significantly enhance the method by helping to distinguish between the relative proportions of net water loss due to evaporation and drainage. Figure 4.3.2 illustrates the determination of a plane of zero potential gradient, the "zero flux" plane, and its use in better defining the proportion of stored water lost by evaporation during a simple soil "dry-down."

Lysimeters. A lysimeter is a device in which a volume of soil, typically 0.5 to 2.0 m in diameter, which may be planted with vegetation, is isolated hydrologically so that leakage $V_L = 0$ in Eq. (4.3.1). It either permits measurement of drainage V_R or makes it zero and, in the case of a weighing lysimeter, the change in water storage V_S is determined by weight difference. Though difficult and expensive to install, lysimeters have extensive and long-established use, primarily in research applications to test alternative measurement techniques or in the calibration of empirical equations to estimate evaporation. Excellent texts on the technical details of lysimeter design and on the value and shortcomings of lysimeter use exist in the literature (e.g., Refs. 1, 117, and particularly 89), to which the reader is referred for more comprehensive description.

Figure 4.3.3 shows an example of a well-designed weighing lysimeter in which vegetation is growing. If evaporation from the lysimeter is to be representative of the surrounding area, it should contain an undisturbed sample of the soil and vegetation.

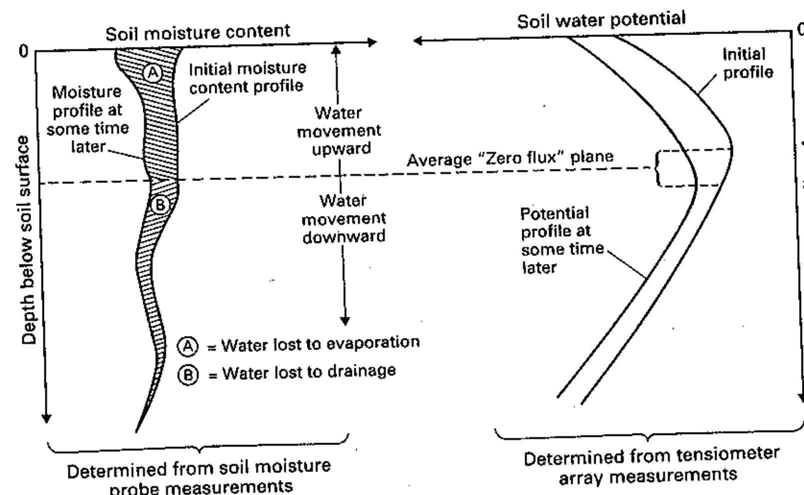

FIGURE 4.3.2 Illustration of the measurement of evaporation using soil moisture depletion supplemented with the determination of an average "zero flux" plane to discriminate between (upward) evaporation and (downward) drainage.

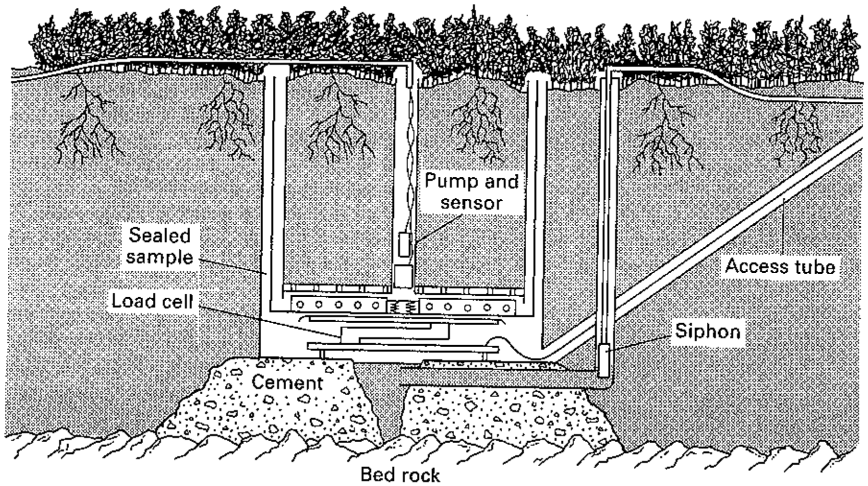

FIGURE 4.3.3 An example of a well-designed weighing lysimeter *(redrawn from Wright.*[133] *Used with permission.)* employing an undisturbed representative sample about 1 m in diameter, with the water status of the soil maintained similar to that of the surrounding area by pumping drainage water.

This means that steps must also be taken to ensure that the thermal, hydrologic, and mechanical properties of the soil are similar to those of surrounding soil, and to establish that the vegetation sample is representative of surrounding vegetation in terms of height, density, and physiological well-being.

Plant Physiological Techniques. Transpiration is the primary component (perhaps 95 percent) of evaporation from dense canopies where little direct solar radiation reaches the ground, or conversely, for sparse vegetation in arid or semiarid climates when the soil surface is very dry. In these particular cases, direct measurement of transpiration gives a worthwhile and cost-effective estimate of total evaporation.

Successful field measurements have been made of transpiration by cutting the stems of the vegetation under water, immersing the cut end in a tank of water, and noting the water uptake,[94] though care is necessary to check that the physiological status of the plant remains representative of the surrounding crop. Measurements of the rate of water flow which do not require cutting the stem are preferable, so methods of observing water flow through plant stems have been developed. These usually involve introducing "tracers" into the stem of the vegetation, sometimes as a pulse of heat to determine sap velocity (e.g., Ref. 25) or as deuterium in the "dilution gauging" method.[22] Success has also been reported[6,100] in deducing the rate of sap flow through its impact on thermal conduction in the stems of herbaceous plants.

4.3.2 Micrometeorological Measurements of Water Vapor Flow into the Atmosphere

Micrometeorological methods of measurement determine evaporation as the flux of water vapor through the air from the evaporating water surface, vegetation, or soil. The measurements are made in the atmosphere, within the turbulent air close to the ground, so that the measured vapor flow rate is a very good approximation to the surface evaporation rate.

There are two broad classes of micrometeorological evaporation measurement: those based on measurements of gradients and those based on measurements of fluctuations. Both rely on the fact that turbulent exchange is the dominant exchange mechanism within the near-surface atmosphere. Since micrometeorological measurements are necessarily made some distance above the ground, and the atmosphere is almost always moving horizontally, the measurements obtained at a particular location are representative of an area some distance upwind. This can be an advantage in that the upwind turbulent mixing helps to produce a value representing the average evaporation over a fairly large area. However, if the measured evaporation is meant to be representative of the particular uniform crop surrounding the instruments, it is necessary that there should be an extensive "fetch" of evaporating surface with essentially identical properties extending upwind from the measurement site for a considerable distance. To test this, the proportion F of the measured evaporation originating from the crop within a specified upwind fetch X_F can be estimated,[41,101] albeit only approximately. In (unstable) daytime conditions

$$F \approx \exp\left(\frac{-6\,(z-d)\,\{\ln[(z-d)/z_o] - 1 + z_o/(z-d)\}}{X_F[1 - z_o/(z-d)]}\right) \tag{4.3.3}$$

here z is the measurement height and $d \simeq 0.67\, h_c$, $z_o \simeq 0.123\, h_c$, and h_c is the average height of the crop. All these heights are in meters.

Methods Based on Measurements of Mean Gradients. The assumption behind these techniques is that above an extensive homogeneous surface the transfer of vapor, momentum, and sensible heat can be described by similar vertical, one-dimensional diffusion equations. It is further assumed that the turbulent diffusion coefficients relating the fluxes of water vapor, sensible heat, and momentum to the respective vertical gradients of humidity, temperature, and wind speed are related to each other in a way which is not determined by characteristics of the surface but rather by characteristics of the turbulent boundary layer itself, and that this relationship is universal, i.e., not dependent on location or crop.

Describing the vertical transport in this way also assumes that evaporation is occurring at a steady rate. In fact this is rarely the case, but the rate of change of evaporation with respect to time is sufficiently slow that average gradients over 20 to 60 min can be successfully used in practice.

Aerodynamic Methods. The basic principle of the aerodynamic method is to assume that the *aerodynamic resistance* (see Sec. 4.2.4), which relates the flow of water vapor to the difference in vapor pressure at heights z_1 and z_2 above the ground, is related in a universally defined and known way to the equivalent aerodynamic resistance to momentum flow between the same two levels. Further, it is assumed that the equation describing the wind-speed profile, and hence momentum flow, above the ground is well known, so that the required difference in aerodynamic resistance between levels z_1 and z_2 can be calculated, as with Eq. (4.2.25).

In practice, the aerodynamic method is rarely applied in this precise way since, were a measurement of the difference in vapor pressure between two heights to be made, it would be preferable and simpler to make an equivalent differential measurement of air temperature over the same height interval, rather than a differential measurement of wind speed. It would then be possible to apply the more accurate energy-balance method described in the next section.

However, the aerodynamic method is used to provide measurement of sensible heat transport, and evaporation is then deduced indirectly from the energy balance using Eq. (4.2.15). This technique is less reliable than other micrometeorological methods, but it has the advantage that the required sensors, two for temperature, two for wind speed, and one for net radiation, are easily available and reasonably cheap and reliable.

Given the required measurements of wind speed u_1 and u_2 and of temperature T_1 and T_2, at the heights z_1 and z_2 *measured relative to the height of the zero plane displacement of the crop,* about 67 percent of crop height; and given the additional measurement of net radiation R_n and perhaps soil heat flux G, it has been shown[54,55] that it is possible to calculate sensible heat adequately using a few simple functions of the differences in temperature, wind speed, and height between z_1 and z_2.

Energy Balance Method. The turbulent diffusion processes responsible for the transport of water vapor and sensible heat through the atmosphere are very similar, but they both differ from those responsible for the transport of momentum. It is therefore a plausible assumption that the aerodynamic resistance which restricts the flow of water vapor and relates that flow rate to the difference in vapor pressure (Δe), between two particular heights, is numerically equal to the resistance which relates the flow of sensible heat to the temperature difference (ΔT) between the same two levels. The *Bowen ratio* β, which is the ratio of the sensible heat H to the latent heat λE, is therefore directly related to the ratio of the differences in temperature and humidity measured between any two heights; thus

$$\beta = \frac{H}{\lambda E} = \gamma \frac{\Delta T}{\Delta e} \tag{4.3.4}$$

the constant γ [see Eq. (4.2.28)] being necessary to account for units.

Using Eq. (4.3.4) it is therefore possible to calculate the ratio of H and λE from differential measurements of temperature and humidity. But, at the same time, by measuring net radiation R_n and soil heat flux G and expressing them as water equivalents, it is possible to also know the sum of these same two energy fluxes from Eq. (4.2.15) by neglecting or estimating the minor terms in Eq. (4.2.16). Solving these two simultaneous equations for the two unknown energy fluxes, the evaporation rate can be calculated from the equation

$$E = \frac{R_n - G}{1 + \gamma(\Delta T/\Delta e)} \qquad \text{mm day}^{-1} \tag{4.3.5}$$

which is sometimes called the *Bowen ratio* method.

Because of the inherent similarity between the diffusion of vapor and sensible heat, the Bowen ratio–energy balance technique is more robust with respect to changes in roughness and topography than is the aerodynamic technique since the profiles of temperature and vapor pressure are affected equally. Moreover, modern systems have been developed[10,36,69] which mechanically and regularly interchange the two temperature and the two humidity sensors between measurement levels, thereby allowing any systematic offset in their calibration to cancel out when the temperature and humidity differences are taken.

The primary practical problem with the Bowen ratio–energy budget technique is that the sign of H often changes in the evening and morning. (Sensible heat flux is usually upward during the day and downward at night.) H, and therefore ΔT, is then zero at the changeover times, so that Eq. (4.3.5) is not defined and applicable at these times. Further, the combination of low (usually negative) values of $(R_n - G)$ at night, and the fact that the two energy fluxes are commonly then in opposite directions, throws suspicion on the usefulness of nighttime measurements of evaporation by the Bowen ratio method.

Eddy Correlation Measurements. Near the surface the mean wind is parallel to the ground, so that the mean vertical wind is zero. However, turbulent eddies within the body of the moving air cause fluctuating vertical movements, both toward and away from the land surface. On average, of course, these fluctuations produce no net vertical movement of the air, but momentarily the air has a vertical velocity w'. If the average specific humidity of the air (in kg of water/kg of air) is $\bar{q}$, then there are similar turbulent fluctuations q' from this mean $\bar{q}$, q' positive meaning greater than average specific humidity and the converse for q' negative.

If w' and q' are simultaneously positive, moister than normal air will be carried away from the ground, and if w' and q' are simultaneously negative, then drier than normal air will move toward the ground. These conditions of positive correlations between w' and q' occur during evaporation; when w' and q' are negatively correlated condensation occurs. The technique for measuring w' and q' and for measuring evaporation from these is called *eddy correlation,* and the evaporation rate E is found as

$$E = 86{,}400\, \overline{\rho_a\, w'\, q'} \qquad \text{mm day}^{-1} \tag{4.3.6}$$

where the overbar denotes a time average. The analogous equation for sensible heat takes the form

$$H = \overline{\rho_a c_p\, w'\, T'} \qquad \text{W m}^2\,\text{s}^{-1} \tag{4.3.7}$$

where T' is the fluctuation in air temperature.

Many practical problems are involved in using the eddy correlation technique. The fluctuations in wind speed, humidity, and temperature can occur over a broad range of frequencies, for instance, some lasting several minutes but others only fractions of a second, and the sensors used to measure w' and q' must have a rapid response. At the same time these sensors have to be co-located, so that they measure the same moving air, yet they should ideally have limited size and be carefully positioned so as not to interfere with the air movements they measure.

It is important to correctly identify the fluctuating components q' and w' and to compute the integrated flux, preferably in real time. Advances in sensor technology and particularly in microprocessors in recent years have allowed associated advances in instrumentation to provide direct evaporation measurement, and integrated measurement systems have evolved (e.g., Ref. 110). Notwithstanding the technical difficulties involved in applying it properly, the eddy correlation technique is the preferred micrometeorological technique on the grounds that it is a direct measurement with minimum theoretical assumptions. Good present-day eddy correlation systems can provide routine evaporation measurements with accuracy in the order of 5 to 10 percent.

Indirect Measurements from Turbulence Statistics. There has been some investigation into measuring evaporation indirectly through its relationships to certain statistical properties of atmospheric turbulence.[16] One such technique is gaining acceptance as viable and simple to apply in semiarid environments, where evaporation is low because of dry soils and difficult to measure otherwise. It can be shown[64,122,129,137] that during the day the standard deviation of air temperature σ_T measured at 5 to

10 m above the ground can be used to calculate the sensible heat flux from

$$H = \rho_a c_p \left[\left(\frac{\sigma_T}{0.92} \right)^3 \frac{0.41\, g\, z}{T + 273.2} \right]^{1/2} \quad \text{W m}^{-2}\,\text{s}^{-1} \tag{4.3.8}$$

where σ_T is the standard deviation of air temperature (in °C) at height z (in m), g is the acceleration due to gravity, and ρ_a is the density of air (in kg m^{-3}) and c_p the specific heat of air (1.01 kJ kg^{-1} K^{-1}). Evaporation can then be deduced from the energy balance using Eqs. (4.2.15) and (4.2.16), given measurements of R_n and G, and neglecting S, P, and A_d.

4.4 METHODS FOR ESTIMATING EVAPORATION

4.4.1 Introductory Comments

There is some distinction between the way evaporation is estimated in hydrologic practice and in hydrologic research. Hydrologists interested in providing realistic models of well-instrumented research catchments, or concerned with the true-to-life description of evaporation in hydrometeorological research, create complex descriptions of the movement of energy and water in the soil-vegetation-atmosphere interface,[44,63,113,127,128] and sometimes also of movement in the lower levels of the atmosphere (e.g., Refs. 13, 67, and 68). Using such complex models generally requires a high level of input data in the form of frequently sampled meteorological variables, and the specification of an extensive set of soil and vegetation parameters for which general values are not yet readily available in the literature. Mainly because of this heavy demand for input data, but partly for historical reasons, such research models are not yet "tools of the trade" for hydrologic practitioners.

Since research models of evaporation do not have the extensive calibration of parameters (or indeed the widespread acceptance) required to recommend them for use by practitioners in a *Handbook of Hydrology,* the understanding generated by modern hydrometeorological research is best applied in a more conservative way. The approach adopted here is to select preferred methods from among the broad range of empirical techniques which practicing hydrologists have proposed over the years and, where relevant and practical, to recommend refinement of such empirical practice.

Accordingly, the conventional approach of estimating evaporation as a two-stage process is retained here. These two stages comprise first estimating a "standard evaporation rate" (see Sec. 4.1.1) and then introducing allowance for different crops and/or soil moisture status as multiplicative factors. Two standard evaporation rates are supported, one for open water surfaces, namely, *potential evaporation* E_o, and one for a well-specified crop, namely, *reference crop evaporation* E_{rc}.

There is one exception to the use of the "two-stage" procedure for estimating evaporation, this being for the case of tall forest vegetation. Although still an active research issue, extensive investigation over the last two decades has demonstrated that, in this case, the difference between evaporation rates when the vegetation is wet and when it is dry is very marked, and so special attention is called for. Forests are therefore treated separately.

4.4.2 Estimating the Energy Available for Evaporation

The energy available at the land surface is normally the primary control on evaporation from open water and a well-watered reference crop. Providing a preliminary estimate (or measurement) of this available energy is necessary for use of the preferred techniques to estimate evaporation described in later sections. How such an estimate of available energy is best provided depends on the type of observational data available.

Table 4.4.1 describes the recommended selection and computation sequence to calculate available energy depending on the data available. This table draws on equations and tables already given but also requires formulas (and associated tables) to provide estimates of the maximum possible sunshine hours N, and of the extraterrestrial solar radiation S_o.

The maximum possible daylight hours[32] can be calculated from

$$N = \frac{24}{\pi} \omega_s \tag{4.4.1}$$

where ω_s is the sunset hour angle (in radians) given by

$$\omega_s = \arccos(-\tan\phi \tan\delta) \tag{4.4.2}$$

where ϕ is the latitude of the site (positive for the Northern hemisphere, negative for the Southern hemisphere) and δ is the solar declination (in radians) given by

$$\delta = 0.4093 \sin\left(\frac{2\pi}{365} J - 1.405 \right) \tag{4.4.3}$$

where J is the Julian day number.

The extraterrestrial solar radiation S_o can be calculated[32] from

$$S_o = 15.392\, d_r (\omega_s \sin\phi \sin\delta + \cos\phi \cos\delta \sin\omega_s) \quad \text{mm day}^{-1} \tag{4.4.4}$$

where d_r is the relative distance between the earth and the sun given by

$$d_r = 1 + 0.033 \cos\left(\frac{2\pi}{365} J \right) \tag{4.4.5}$$

Equations (4.4.1) and (4.4.4) provide estimates of the maximum possible daylight hours and extraterrestrial solar radiation which are good to about 0.1 h and 0.1 mm day^{-1}, respectively, for latitudes between 55°S and 55°N. As a check on computer code to evaluate N and S_o, their April 15 values ($J = 105$) at latitudes 30°N, 0, and 30°S are 12.7, 12.0, and 11.3 h, and 15.0, 15.1, and 11.2 mm day^{-1}, respectively.

4.4.3 Computing Other Inputs for Evaporation Estimates

Vapor-Pressure Deficit. Preferred techniques for estimating evaporation require a value of the vapor-pressure deficit D, the difference between saturated vapor pressure e_s and ambient vapor pressure e, averaged over the period for which the estimate is made. On rare occasions the true average vapor-pressure deficit is available—based on hourly values from an automatic weather station perhaps—but more usually it has to be estimated from climatological records.

TABLE 4.4.1 Selection and Computation Sequence for Estimating the Energy Available for Evaporation

1	Are local measurements of net radiation (R_n in MJ m^{-2} day^{-1}) available?		
	YES:	(i)	Divide by λ [Eq. (4.2.1)] to give R_n in mm day^{-1}.
		(ii)	Go to 5(a).
	NO:		Continue with 2(a).
2(a)	Are local records of fractional cloud cover (n/N) available?		
	YES:		Go to 3(a).
	NO:		Continue with 2(b).
2(b)	Local records of sunshine hours (n) available?		
	YES:	(i)	Compute (n/N); N from Eq. (4.4.1).
		(ii)	Go to 3(a).
	NO:		Continue with 2(c).
2(c)	Can n or n/N be estimated from regional records?		
	YES:	(i)	Proceed as 2(a) or 2(b).
		(ii)	Recognize increased uncertainty in (n/N).
		(iii)	Go to 3(a).
	NO:		Select pan- or temperature-based evaporation estimate.
3(a)	Local measurements of solar radiation (S_t in MJ m^{-2} day^{-1}) available?		
	YES:	(i)	Divide by λ [Eq. (4.2.1)] to give water equivalent.
		(ii)	Go to 3(c).
	NO:		Continue with 3(b).
3(b)	Locally calibrated angstrom coefficients (a_s, b_s) available?		
	YES:		Select a_s and b_s from available values.
	NO:		Set $a_s = 0.25$; $b_s = 0.50$.
	THEN:	(i)	Obtain value of extraterrestrial radiation (S_o) from Eq. (4.4.4).
		(ii)	Compute S_t from Eq. (4.2.6).
		(iii)	Continue with 3(c).
3(c)	Local measurements of land cover albedo (α) available?		
	YES:		Select value of α from available measurements.
	NO:		Estimate α using Table 4.2.2.
	THEN:	(i)	Compute net solar radiation from Eq. (4.2.5).
		(ii)	Continue with 4(a).
4(a)	Locally calibrated emissivity coefficients [a_e, b_e; Eq. (4.2.8)] available?		
	YES:		Select a_e and b_e from available values.
	NO:		Set $a_e = 0.34$; $b_e = -0.14$.
	THEN:		Continue with 4(b).
4(b)	Measurements of dew point temperature available?		
	YES:	(i)	Obtain vapor pressure e_d at dew point temperature from Eq. (4.2.2) or Table 4.2.1.
		(ii)	Compute ϵ' from Eq. (4.2.8).
		(iii)	Go to 4(d).
	NO:		Continue with 4(c).
4(c)	Measurements of minimum air temperature available?		
	YES:	(i)	Set dew point to minimum temperature; obtain e_d from Eq. (4.2.2) or Table 4.2.1.
		(ii)	Compute ϵ' from Eq. (4.2.8).
	NO:		Compute ϵ' from Eq. (4.2.9).
	THEN:		Continue with 4(d).
4(d)	Locally calibrated cloudiness coefficients [a_c, b_c; Eq. (4.2.10)] available?		
	YES:		Select a_c and b_c from available values.
	NO:		Set $a_c = 1.35$; $b_c = -0.35$ in arid areas or $a_c = 1.00$; $b_c = 0.00$ in humid areas.

TABLE 4.4.1 Selection and Computation Sequence for Estimating the Energy Available for Evaporation *(Continued)*

	THEN:	(i)	Compute clear sky solar radiation S_{to} as the value given by Eq. (4.2.6) with (n/N) set to ~~zero~~. one
		(ii)	Compute the cloudiness factor (f) from Eq. (4.2.10).
		(iii)	Compute net long-wave radiation from Eq. (4.2.7).
		(iv)	Compute net radiation from Eq. (4.2.13).
		(v)	Continue with 5(a).
5(a)	Estimate of available energy for open water surface required?		
	YES:		Go to 5(b).
	NO:		Go to 5(c).
5(b)	Data to estimate advected energy [A_h; Eq. (4.2.20)] available?		
	YES:	(i)	Compute A_h from Eq. (4.2.20).
		(ii)	Energy available for evaporation $A = R_n + A_h$.
	NO:		Energy available for evaporation $A = R_n$.
	THEN:		Energy estimation complete.
5(c)	Measurements or data to estimate soil heat flux G available?		
	YES:	(i)	Obtain G from measurements, or estimate from Eq. (4.2.18) or (4.2.19).
		(ii)	Energy available for evaporation $A = R_n - G$.
	NO:		Energy available for evaporation $A = R_n$.
	THEN:		Energy estimation complete.

Since saturated vapor pressure is not a linear function of temperature [see Eq. (4.2.2)] the particular procedure used to estimate vapor-pressure deficit from such climatological records can affect the estimated value (by as much as 30 percent), particularly in arid environments where the daily temperature cycle is often large. In general terms, and if possible, computing vapor-pressure deficit at the measured maximum and minimum temperature separately, and then taking the average of these deficit values, provides a better estimate of the true daily average deficit than averaging temperatures (or relative humidities) first and then computing the deficit.

Climatological humidity data are reported either (1) as relative humidity (RH_{max} and RH_{min}, in percentage); or (2) as daily average dry- and wet-bulb temperatures (T_d and T_w, in °C); or (3) as a daily average dew-point temperature (T_{dew}, in °C). The time of measurement is important but is often not given. Fortunately the actual vapor pressure of the air is fairly constant, and even one measurement per day may suffice, particularly if this measurement is made early in the day.

If a true daily average vapor-pressure deficit $\bar{D}$ is not available and an estimate from climatological data is required, the following averaging procedures are recommended for the three different humidity data availabilities given above.

1. *Relative Humidity.* Data given: T_{max}, T_{min}, RH.

$$\bar{D} = \left[\frac{e_s(T_{max}) + e_s(T_{min})}{2}\right]\frac{(1 - RH)}{100} \quad \text{kPa} \tag{4.4.6}$$

with $e_s(T_{max})$ and $e_s(T_{min})$ from Eq. (4.2.2) or Table 4.2.1. If more than one value of relative humidity is available, RH is the average value.

2. *Wet- and Dry-Bulb Temperature.* Data given: T_{max}, T_{min}, T_{dry}, T_{wet}.

$$\bar{D} = \frac{e_s(T_{max}) + e_s(T_{min})}{2} - e \quad \text{kPa} \tag{4.4.7}$$

with $e_s(T_{max})$ and $e_s(T_{min})$ from Eq. (4.2.2) or Table 4.2.1; and e taken from Table 4.4.2 for *(a)* aspirated and *(b)* unaspirated psychrometers, respectively. If more

TABLE 4.4.2a Vapor Pressure (in kPa) from Dry- and Wet-Bulb Temperature Data (in °C) for an Aspirated Psychrometer

Wet-bulb depression, °C (altitude < 1000 m)												Dry bulb, °C	Wet-bulb depression, °C (altitude > 1000 m)											
0	2	4	6	8	10	12	14	16	18	20	22		0	2	4	6	8	10	12	14	16	18	20	22
7.38	6.49	5.68	4.92	4.22	3.58	2.98	2.43	1.92	1.44	1.01	0.60	40	7.38	6.52	5.71	4.98	4.30	4.18	3.10	2.56	2.07	1.62	1.20	0.81
6.63	5.81	5.05	4.36	3.71	3.11	2.56	2.05	1.58	1.14	0.73		38	6.63	5.82	5.09	4.41	3.79	3.67	2.68	2.18	1.73	1.32	0.92	0.57
5.94	5.19	4.49	3.84	3.25	2.69	2.18	1.71	1.27	0.86	0.49		36	5.94	5.21	4.52	3.90	3.33	3.21	2.30	1.84	1.43	1.04	0.68	0.35
5.32	4.62	3.98	3.38	2.83	2.32	1.84	1.40	1.00	0.62			34	5.32	4.64	4.01	3.44	2.91	2.41	1.96	1.54	1.15	0.80	0.46	0.15
4.75	4.11	3.51	2.96	2.45	1.98	1.54	1.13	0.70	0.40			32	4.75	4.13	3.55	3.02	2.53	2.07	1.66	1.26	0.91	0.58	0.26	
4.24	3.65	3.09	2.58	2.11	1.67	1.26	0.88	0.53				30	4.24	3.67	3.13	2.64	2.19	1.77	1.38	1.02	0.69	0.38	0.09	
3.78	3.23	2.72	2.24	1.80	1.40	1.02	0.67	0.34				28	3.78	3.25	2.75	2.30	1.89	1.49	1.14	0.80	0.49	0.21		
3.36	2.85	2.38	1.94	1.53	1.15	0.80	0.47	0.16				26	3.36	2.87	2.41	2.00	1.61	1.25	0.92	0.60	0.32	0.05		
2.98	2.51	2.07	1.66	1.28	0.93	0.60	0.29					24	2.98	2.53	2.11	1.72	1.39	1.03	0.72	0.43	0.16			
2.64	2.20	1.80	1.42	1.06	0.74	0.43	0.14					22	2.64	2.23	1.83	1.43	1.15	0.83	0.55	0.27	0.02			
2.34	1.93	1.55	1.20	0.87	0.56	0.27						20	2.34	1.95	1.59	1.26	0.95	0.66	0.39	0.13				
2.06	1.68	1.33	1.00	0.69	0.41	0.14						18	2.06	1.71	1.37	1.06	0.78	0.50	0.25	0.01				
1.82	1.46	1.14	0.83	0.54	0.27							16	1.82	1.49	1.17	0.89	0.62	0.36	0.13					
1.60	1.27	0.96	0.67	0.40	0.15							14	1.60	1.29	1.00	0.73	0.48	0.24	0.03					
1.40	1.09	0.81	0.53	0.28								12	1.40	1.12	0.84	0.59	0.36	0.14						
1.23	0.94	0.67	0.41	0.17								10	1.23	0.96	0.70	0.47	0.26	0.04						
1.07	0.80	0.55	0.31	0.08								8	1.07	0.82	0.58	0.37	0.16							
0.93	0.68	0.44	0.21									6	0.93	0.70	0.48	0.27	0.07							
0.81	0.57	0.34	0.16									4	0.81	0.60	0.38	0.18								
0.71	0.48	0.28	0.08									2	0.71	0.50	0.29	0.10								
0.61	0.40	0.20										0	0.61	0.41	0.21									

Source: After Doorenbos and Pruitt.[30] Used with permission.

TABLE 4.4.2b Vapor Pressure (in kPa) from Dry- and Wet-Bulb Temperature Data (in °C) for a Nonventilated Psychrometer

Wet-bulb depression, °C (altitude < 1000 m)												Dry bulb, °C	Wet-bulb depression, °C (altitude > 1000 m)											
0	2	4	6	8	10	12	14	16	18	20	22		0	2	4	6	8	10	12	14	16	18	20	22
7.38	6.47	5.62	4.84	4.12	3.44	2.82	2.24	1.70	1.20	0.74	0.30	40	7.38	6.49	5.67	4.91	4.20	3.56	2.96	2.41	1.89	1.41	0.98	0.56
6.63	5.78	5.00	4.28	3.60	2.98	2.40	1.86	1.36	0.90	0.46	0.06	38	6.63	5.80	5.05	4.34	3.69	3.10	2.54	2.03	1.55	1.11	0.70	0.32
5.94	5.16	4.44	3.76	3.14	2.56	2.02	1.52	1.06	0.62	0.22		36	5.94	5.18	4.48	3.83	3.23	2.68	2.12	1.69	1.25	0.83	0.46	0.10
5.32	4.59	3.92	3.30	2.72	2.18	1.68	1.22	0.78	0.38			34	5.32	4.61	3.97	3.37	2.81	2.30	1.82	1.39	0.97	0.59	0.24	
4.75	4.08	3.46	2.88	2.34	1.84	1.38	0.94	0.54	0.16			32	4.75	4.10	3.51	2.95	2.43	1.96	1.52	1.11	0.73	0.37	0.04	
4.24	3.62	3.04	2.50	2.00	1.54	1.10	0.70	0.32				30	4.24	3.64	3.09	2.57	2.09	1.66	1.24	0.87	0.51	0.17		
3.78	3.20	2.66	2.16	1.70	1.26	0.86	0.48	0.12				28	3.78	3.22	2.71	2.23	1.79	1.38	1.00	0.65	0.31			
3.36	2.82	2.32	1.86	1.42	1.02	0.64	0.28					26	3.36	2.84	2.37	1.93	1.51	1.14	0.78	0.45	0.14			
2.98	2.48	2.02	1.58	1.19	0.80	0.44	0.11					24	2.98	2.50	2.07	1.65	1.27	0.92	0.58	0.28				
2.64	2.18	1.74	1.34	0.96	0.60	0.27						22	2.64	2.20	1.79	1.41	1.05	0.72	0.41	0.12				
2.34	1.90	1.50	1.12	0.76	0.43	0.11						20	2.34	1.92	1.55	1.19	0.85	0.55	0.25					
2.06	1.66	1.28	0.92	0.59	0.27							18	2.06	1.68	1.33	0.99	0.68	0.39	0.11					
1.82	1.44	1.08	0.75	0.43	0.14							16	1.82	1.46	1.13	0.82	0.52	0.25						
1.60	1.24	0.91	0.59	0.30	0.01							14	1.60	1.26	0.96	0.66	0.38	0.13						
1.40	1.07	0.75	0.46	0.17								12	1.40	1.09	0.80	0.52	0.26	0.03						
1.23	0.91	0.61	0.33	0.07								10	1.23	0.93	0.67	0.40	0.16							
1.07	0.77	0.49	0.23									8	1.07	0.79	0.54	0.30	0.06							
0.93	0.65	0.39	0.15									6	0.93	0.67	0.44	0.20								
0.81	0.55	0.29	0.09									4	0.81	0.57	0.34	0.11								
0.71	0.45	0.23										2	0.71	0.47	0.25	0.03								
0.61	0.37	0.15										0	0.61	0.38	0.17									

Source: After Doorenbos and Pruitt.[30] Used with permission.

than one pair of dry- and wet-bulb temperatures are available, e is the average value derived from these.

3. *Dew-Point Temperature.* Data given: T_{max}, T_{min}, T_{dew}.

$$\overline{D} = \frac{e_s(T_{max}) + e_s(T_{min})}{2} - e(T_{dew}) \qquad \text{kPa} \tag{4.4.8}$$

with $e_s(T_{max})$, $e_s(T_{min})$, and $e_s(T_{dew})$ from Eq. (4.2.2) or Table 4.2.1.

Adjustments for Measurement Heights. The preferred techniques for estimating evaporation given in later sections are appropriate for measured vapor-pressure deficit $\overline{D}$ and wind speed U_2 at a height of 2 m. For reference crop evaporation E_{rc} the equivalent value of the aerodynamic resistance r_a alters if the measurement height of either humidity or wind speed is other than 2 m. However, this can be allowed for by adjusting the effective value of wind speed used in Eq. (4.2.31) and the estimating equations below to U_2', this value being given by the equation

$$\frac{U_2'}{U_2} = \frac{34.9648}{\ln\left(\dfrac{z_e - 0.08}{0.001476}\right) \ln\left(\dfrac{z_u - 0.08}{0.01476}\right)} \tag{4.4.9}$$

where z_e and z_u are the actual heights of the humidity and wind speed measurements, respectively. For example, $U_2'/U_2 = 1.116$ for $z_e = 1$ m and $z_u = 2$ m, and $U_2'/U_2 = 0.749$ for $z_e = 2$ m and $z_u = 10$ m.

Equation (4.4.9) may also be adequate to correct wind speeds for the purposes of estimating potential evaporation rates for open water surfaces, bearing in mind the empirical and approximate nature of Eqs. (4.2.30) and (4.2.33).

4.4.4 Estimating the Evaporation Rate from Open Water

The preferred method for estimating the rate of evaporation from open water is from Eq. (4.2.30), which is here rewritten in the form

$$E_p = F_p^1 A + F_p^2 \overline{D} \qquad \text{mm day}^{-1} \tag{4.4.10}$$

where A is the energy available for evaporation (in mm day^{-1}), given by $A = (R_n + A_h)$, and estimated following the procedure given in Sec. 4.4.2; and $\overline{D}$ is the (average) vapor-pressure deficit (in kPa) calculated as in Sec. 4.4.3.

The coefficient F_p^1 is a function of temperature and the elevation of the site:

$$F_p^1 = \frac{\Delta}{\Delta + \gamma} \tag{4.4.11}$$

in which Δ is given by substituting e_s from Eq. (4.2.2) into Eq. (4.2.3); and γ by substituting λ from Eq. (4.2.1) into Eq. (4.2.28); with the atmospheric pressure P (in kPa), estimated from

$$P = 101.3\left(\frac{293 - 0.0065Z}{293}\right)^{5.256} \tag{4.4.12}$$

where Z is the elevation of the site (in m).

TABLE 4.4.3 Values of Parameters in Evaporation Estimation Eqs. (4.4.10), (4.4.14), and (4.4.17) for Two Elevations above Sea Level, and Sample Values of Mean Air Temperature and Wind Speed

Elevation Z, m	Temperature T, °C	Wind speed U_2, m s^{-1}	F_p^1	F_p^2	F_{rc}^1	F_{rc}^2	F_{pt}^{humid}	F_{pt}^{arid}
0	10	3	0.553	3.028	0.383	2.937	0.696	0.962
0	10	6	0.553	4.895	0.293	4.495	0.696	0.962
0	30	3	0.781	1.505	0.643	1.588	0.985	1.360
0	30	6	0.781	2.433	0.546	2.697	0.985	1.360
1000	10	3	0.582	2.832	0.411	2.803	0.733	1.012
1000	10	6	0.582	4.578	0.318	4.336	0.733	1.012
1000	30	3	0.801	1.371	0.670	1.470	1.010	1.394
1000	30	6	0.801	2.216	0.575	2.524	1.010	1.394

The coefficient F_p^2 is a function of temperature, wind speed, and the elevation of the site:

$$F_p^2 = \left(\frac{\gamma}{\Delta + \gamma}\right)\frac{6.43(1 + 0.536U_2)}{\lambda} \tag{4.4.13}$$

in which Δ and γ are given as for Eq. (4.4.11); U_2 is the wind speed measured at 2 m [or the effective value calculated from Eq. (4.4.9) if necessary]; and λ is given by Eq. (4.2.1). Computer code to calculate F_p^1 and F_p^2 can be checked using the sample values given in Table 4.4.3.

The allowance for atmospheric diffusion (see Sec. 4.2.5) implicit in F_p^2 is relevant to open water surfaces with reasonable small surface area, and Eq. (4.4.10) is therefore expected to provide weekly or monthly estimates of the evaporation rate from shallow, ground-level evaporation pans (or small ponds or lakes) which are good to 5 to 10 percent or 0.5 mm day^{-1}, whichever is greater. The effective value of the aerodynamic resistance for much larger expanses of water is larger (see Sec. 4.2.7), and the evaporation rate is therefore reduced. Equation (4.4.10) might therefore systematically overestimate the evaporation for very large lakes by approximately 10 to 15 percent.

Of the alternative techniques for estimating open water evaporation, the Kimberly-Penman equation,[56,134] given earlier as Eq. (4.2.33), has been shown[56] to have marginal advantage over Eq. (4.4.10) in semiarid environments but is marginally worse in humid environments. If not all of the climatological data are available to allow a calculation of E_p from either Eq. (4.4.10) or Eq. (4.2.33), the use of the same secondary estimation techniques as for reference crop evaporation is recommended based on radiation, pan, or temperature data (see Sec. 4.4.5). Estimates based on radiation, however, should use measurements or estimates of the energy available for evaporation relevant to open water (as opposed to grassed) surfaces; see Sec. 4.4.2.

4.4.5 Estimating the Evaporation Rate of the Reference Crop

Preferred Method. The preferred method for estimating the rate of evaporation from the reference crop or short actively growing grass (see Sec. 4.1.1 for definition) is from Eq. (4.2.31), which is here rewritten in the form

$$E_{rc} = F^1_{rc} A + F^2_{rc} \overline{D} \qquad \text{mm day}^{-1} \tag{4.4.14}$$

where A is the energy available for evaporation (in mm day^{-1}), given by $A = (R_n + A_h)$, and estimated following the procedure given in Sec. 4.4.2; and $\overline{D}$ is the (average) vapor-pressure deficit (in kPa) calculated as in Sec. 4.4.3.

The coefficient F^1_{rc} is a function of temperature, wind speed, and the elevation of the site:

$$F^1_{rc} = \frac{\Delta}{\Delta + \gamma^*} \tag{4.4.15}$$

in which Δ is given by substituting e_s from Eq. (4.2.2) into Eq. (4.2.3); and γ^* is given by Eq. (4.2.32), with γ obtained by substituting Eq. (4.2.1) into Eq. (4.2.28) and P taken from Eq. (4.4.12).

The coefficient F^2_{rc} is similarly a function of temperature, wind speed, and the elevation of the site:

$$F^2_{rc} = \left(\frac{\gamma}{\Delta + \gamma^*}\right) \frac{900\ U_2}{T + 275} \tag{4.4.16}$$

the required inputs being derived as for Eq. (4.4.15). Computer code to calculate F^1_{rc} and F^2_{rc} can be checked using the sample values given in Table 4.4.3.

Errors in estimating the evaporation from the precisely defined reference crop using Eq. (4.4.14) do not primarily arise because of the empirical values involved, since these are related to the physically-based values which control evaporation rate in the Penman-Monteith equation. Rather, they arise through differences between these values and those relevant to the particular crop for which estimates are made. Studies[56] suggest differences of the order 5 to 7 percent or 0.5 mm day^{-1} may arise.

Radiation-Based Estimates. The preferred radiation-based method for estimating reference crop evaporation is from Eq. (4.2.37), which is here rewritten in the form

$$E_{rc} = F_{pt} A \qquad \text{mm day}^{-1} \tag{4.4.17}$$

$F_{pt} = \alpha[\Delta/(\Delta + \gamma)]$, with $\alpha = 1.74$ for arid regions and $\alpha = 1.26$ for all other (humid) locations [see Eqs. (4.2.38) and (4.2.39)]. Arid regions, in this context, are defined as having relative humidity of less than 60 percent in the month with peak evaporation. The value of $(R_n - G)$ is estimated following the procedure given in Sec. 4.4.2.

Computer code to calculate F_{pt} for humid and arid locations can be checked using the sample values given in Table 4.4.3. Estimates using this method are prone to errors of the order 15 percent or 0.75 mm day^{-1}, whichever is greater, and should be made only for periods of 10 days or longer.

Other radiation-based estimation methods, especially those given by Turc[125] and Doorenbos and Pruitt,[30] are also in common use and are described in Sec. 4.2.6.

Pan-Based Estimates. The preferred pan-based method for estimating reference crop evaporation is from Eq. (4.3.2), with values of pan coefficients for Class A pans from Table 4.3.1. Estimated errors in using this technique are typically of the order 10 to 15 percent or 1 mm day^{-1}, whichever is greater; for regions where dry winds predominate, or where the upwind fetches are low, the errors may well be twice as large.

Temperature-Based Estimates. Estimating evaporation from temperature data is not recommended, except when lack of other data means this is the only option available. In these conditions the Hargreaves equation [Eq. (4.2.44)] is the preferred technique and Ref. 56 may provide estimates with errors in the order 10 to 15 percent or 1 mm day^{-1}, whichever is greater.

Other more complex temperature-based techniques are still in common use, in particular the Doorenbos and Pruitt version of the Blaney-Criddle method; see Eq. (4.2.45). Comparison[56] suggests the additional complexity in this provides a marginally inferior estimate to that given by the Hargreaves equation.

4.4.6 Estimating the Evaporation Rate of Other Crops

It is the actual evaporation which is most often required and, in principle, this could be estimated directly from Eq. (4.2.27) if there are values of r_s and r_a available which are appropriate to the particular crop for which estimates are required. In practice this is rarely the case except in research application, and it is therefore common practice to estimate first the evaporation rate for the reference crop (for which r_s and r_a are prescribed), and then multiply this rate by an additional factor; thus

$$E = K_c E_{rc} \qquad \text{mm day}^{-1} \tag{4.4.18}$$

The factor K_c in this equation is called the *crop coefficient* and, from a comparison with Eqs. (4.2.27) and (4.2.31), it is clearly a complex factor. It contains a significant dependence on the effective average surface resistance of the actual crop (relative to the reference crop), and this is the primary influence in dry conditions, but it also depends on vegetation height through r_a. Moreover, K_c has some dependence on meteorological variables, i.e., on temperature (through Δ), on wind speed (through r_a), and on rainfall (through r_s, indirectly, depending on the amount of time the canopy is wet). Clearly the value of crop coefficient will depend not only on the crop and its stage of development, but also in part on the average climate in which any empirical calibration is carried out.

Irrigated Field Crops. In practice many evaporation estimation applications concern the irrigation of agricultural crops. The objective is usually to supply water which is adequate, in that it does not limit growth, but not excessive, so that the soil surface is not waterlogged. In this case the *potential crop coefficient* K_{co} is relevant, this being defined from the equation

$$E = K_{co} E_{rc} \qquad \text{mm day}^{-1} \tag{4.4.19}$$

It is likely that K_{co} is less variable than K_c in moving from one location to the next, since it is a purer measure of stomatal resistance, which in turn is less variable since the soil moisture deficit remains small. (It will of course still have some local meteorological dependence through Δ and r_a.)

Considerable research has been directed toward defining K_{co} as a function of time for different crops. As might be expected for annual agricultural crops, with which it is often used, there is a pronounced seasonal variation of the type illustrated schematically in Fig. 4.4.1. This figure can be used to provide estimates of the seasonal variation in potential crop coefficient[30] for the range of (annual) field crops listed in Table 4.4.4 as follows:

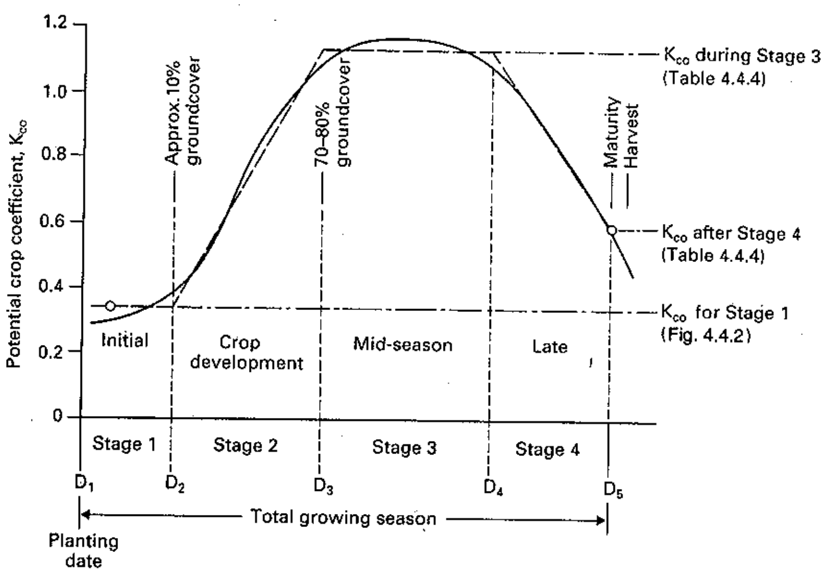

FIGURE 4.4.1 Schematic diagram of the seasonal changes in potential crop coefficient K_{co} for an irrigated field crop *(redrawn from Doorenbos and Pruitt.[30] Used with permission.)* illustrating four growth stages (initial, crop development, midseason, late) in the total growing season defined relative to the planting date D_1 and terminating at the dates D_2, D_3, D_4, and D_5, respectively. The value of K_{co} during the initial Stage 1 is taken from Fig. 4.4.2, and the values during Stage 3 and after D_5 are taken from Table 4.4.4. Intervening values during Stages 2 and 4 are determined by interpolation.

1. Establish the planting or sowing date and, if possible, determine the total growing season and length of the individual crop development stages from local information; otherwise estimates of the typical growing season and of the proportion of this at each growth stage are given in Table 4.4.4. Use these to determine the dates D_2, D_3, D_4, and D_5 for the time series of K_{co} (see Fig. 4.4.1) relative to the planting date D_1.
2. The (constant) value of K_{co} for Stage 1 is a function of the reference crop evaporation at the time of sowing and the average interval between rain or irrigation at this time. Determine this value from Fig. 4.4.2.
3. For a given crop growing in a given climate (humidity and wind), the (constant) value of K_{co} for Stage 3 (i.e., midseason, from date D_3 to D_4) is given in Table 4.4.4, as is the value of K_{co} at maturity or harvest (after Stage 4, at time D_5).
4. The full seasonal variation in K_{co} is then obtained by interpolating between the values at D_2 and D_3, and those at D_4 and D_5.

An estimate of the seasonal variation in E, and thus of the irrigation demand, can be made through the season by introducing these time-dependent estimates of K_{co} into Eq. (4.4.19), along with estimates of E_{rc}.

Irrigated Grasslike Crops. For irrigated alfalfa, grasses, clover, or grass-legumes successively cut for fodder throughout the season, or for well-irrigated and well-fertilized (grass, grass-legumes, or alfalfa) pastures, it is generally sufficient[30] to use

TABLE 4.4.4 For a Range of Irrigated Field Crops, the Typical Total Growing Season in Days; Representative Proportions of This Growing Season at Each of the Growth Stages Illustrated in Fig. 4.4.1; and Recommended Values of K_{co} During Stage 3 and After Stage 4 in Different (Wind and Humidity) Climates

Crop	Typical growing season, days	Fraction of stage time at growth stage				K_{co} during Stage 3				K_{co} after Stage 4			
						$RH_{min} > 70\%$		$RH_{min} < 20\%$		$RH_{min} > 70\%$		$RH_{min} < 20\%$	
						Wind, m s^{-1}		Wind, m s^{-1}		Wind, m s^{-1}		Wind, m s^{-1}	
		1	2	3	4	0–5	5–8	0–5	5–8	0–5	5–8	0–5	5–8
Artichokes (perennial)	310–360	0.09	0.12	0.70	0.09	0.95	0.95	1.00	1.05	0.90	0.90	0.95	1.00
Barley	120–150	0.12	0.20	0.44	0.24	1.05	1.10	1.15	1.20	0.25	0.25	0.20	0.20
Beans (green)	75–90	0.22	0.33	0.33	0.12	0.95	0.95	1.00	1.05	0.85	0.85	0.90	0.90
Beans (dry)/Pulses	95–110	0.16	0.25	0.40	0.19	1.05	1.10	1.15	1.20	0.30	0.30	0.25	0.25
Beets (table)	70–90	0.24	0.35	0.29	0.12	1.00	1.00	1.05	1.10	0.90	0.90	0.95	1.00
Carrots	100–150	0.18	0.27	0.39	0.16	1.00	1.05	1.10	1.15	0.70	0.75	0.80	0.85
Castor beans	180	0.14	0.22	0.36	0.28	1.05	1.10	1.15	1.20	0.50	0.50	0.50	0.50
Celery	125–180	0.16	0.27	0.46	0.11	1.00	1.05	1.10	1.15	0.90	0.95	1.00	1.05
Corn (sweet)	80–110	0.23	0.29	0.37	0.11	1.05	1.10	1.15	1.20	0.95	1.00	1.05	1.10
Corn (grain)	125–180	0.17	0.28	0.33	0.22	1.05	1.10	1.15	1.20	0.55	0.55	0.60	0.60
Cotton	180–195	0.16	0.27	0.31	0.26	1.05	1.15	1.20	1.25	0.65	0.65	0.65	0.70
Crucifers	80–95	0.24	0.38	0.26	0.12	0.95	1.00	1.05	1.10	0.80	0.85	0.90	0.95
Cucumber	105–130	0.19	0.28	0.38	0.15	0.90	0.90	0.95	1.00	0.70	0.70	0.75	0.80
Eggplant	130–140	0.21	0.32	0.30	0.17	0.95	1.00	1.05	1.10	0.80	0.85	0.85	0.90
Flax	150–220	0.15	0.21	0.39	0.25	1.00	1.05	1.10	1.15	0.25	0.25	0.20	0.20
Grain (small)	150–165	0.14	0.20	0.40	0.26	1.05	1.10	1.15	1.20	0.30	0.30	0.25	0.25
Lentil	150–170	0.14	0.20	0.41	0.25	1.05	1.10	1.15	1.20	0.30	0.30	0.25	0.25
Lettuce	75–140	0.26	0.37	0.27	0.10	0.95	0.95	1.00	1.05	0.90	0.90	0.90	1.00
Melons	120–160	0.20	0.28	0.37	0.15	0.95	0.95	1.00	1.05	0.65	0.65	0.75	0.75
Millet	105–140	0.14	0.23	0.39	0.24	1.00	1.05	1.10	1.15	0.30	0.30	0.25	0.25
Oats	120–150	0.12	0.20	0.44	0.24	1.05	1.10	1.15	1.20	0.25	0.25	0.20	0.20
Onion (dry)	150–210	0.10	0.17	0.49	0.24	0.95	0.95	1.05	1.10	0.75	0.75	0.80	0.85

(Continued)

TABLE 4.4.4 For a Range of Irrigated Field Crops, the Typical Total Growing Season in Days; Representative Proportions of This Growing Season at Each of the Growth Stages Illustrated in Fig. 4.4.1; and Recommended Values of K_{co} During Stage 3 and After Stage 4 in Different (Wind and Humidity) Climates *(Continued)*

Crop	Typical growing season, days	Fraction of stage time at growth stage				K_{co} during Stage 3				K_{co} after Stage 4			
						$RH_{min} > 70\%$		$RH_{min} < 20\%$		$RH_{min} > 70\%$		$RH_{min} < 20\%$	
						Wind, m s^{-1}		Wind, m s^{-1}		Wind, m s^{-1}		Wind, m s^{-1}	
		1	2	3	4	0–5	5–8	0–5	5–8	0–5	5–8	0–5	5–8
Onion (green)	70–95	0.29	0.45	0.17	0.09	0.95	0.95	1.00	1.05	0.95	0.95	1.00	1.05
Groundnuts	130–140	0.22	0.30	0.30	0.18	0.95	1.00	1.05	1.10	0.55	0.55	0.60	0.60
Peas	90–100	0.21	0.26	0.37	0.16	1.05	1.10	1.15	1.20	0.95	1.00	1.05	1.10
Peppers (fresh)	120–125	0.22	0.29	0.33	0.16	0.95	1.00	1.05	1.10	0.80	0.85	0.85	0.90
Potato	105–145	0.21	0.25	0.33	0.21	1.05	1.10	1.15	1.20	0.70	0.70	0.75	0.75
Radishes	35–40	0.20	0.27	0.40	0.13	0.80	0.80	0.85	0.90	0.75	0.75	0.80	0.85
Safflower	125–190	0.17	0.27	0.35	0.21	1.05	1.10	1.15	1.20	0.25	0.25	0.20	0.20
Sorghum	120–130	0.16	0.27	0.33	0.24	1.00	1.05	1.10	1.15	0.50	0.50	0.55	0.55
Soybeans	135–150	0.14	0.21	0.46	0.19	1.00	1.05	1.10	1.15	0.45	0.45	0.45	0.45
Spinach	60–100	0.27	0.31	0.34	0.08	0.90	0.95	1.00	1.05	0.90	0.90	0.95	1.00
Squash	90–100	0.24	0.34	0.26	0.16	0.90	0.90	0.95	1.00	0.70	0.70	0.75	0.80
Sugar beet	160–230	0.18	0.27	0.33	0.22	1.05	1.10	1.15	1.20	0.90	0.95	1.00	1.00
Sunflower	125–130	0.17	0.28	0.36	0.19	1.05	1.10	1.15	1.20	0.40	0.40	0.35	0.35
Tomato	135–180	0.20	0.28	0.33	0.19	1.05	1.10	1.20	1.25	0.60	0.60	0.65	0.65
Wheat	120–150	0.12	0.20	0.44	0.24	1.05	1.10	1.15	1.20	0.25	0.25	0.20	0.20

Source: Derived from Doorenbos and Pruitt (Ref. 30, Tables 21 and 22). Used with permission.

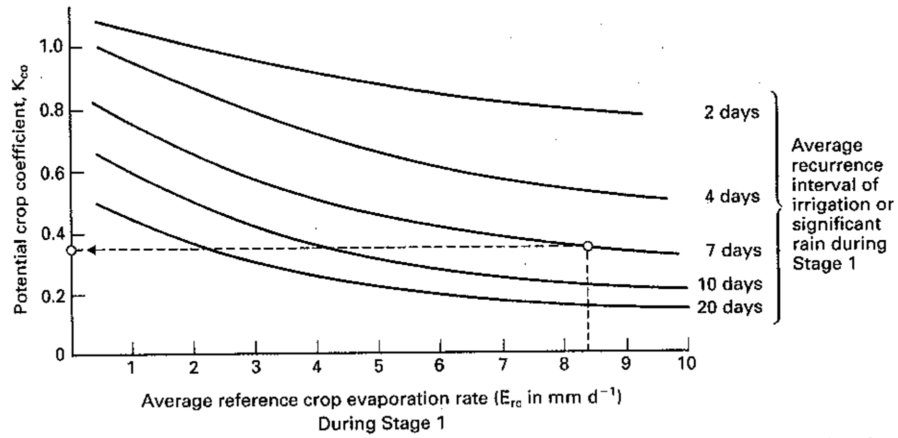

FIGURE 4.4.2 The potential crop coefficient K_{co} to be applied during Stage 1 (see text and Fig. 4.4.1) based on the average reference crop evaporation rate E_{rc} during this time and the estimated recurrence interval between significant rainfall or irrigation *(redrawn from Doorenbos and Pruitt.[30] Used with permission.)*. The example shown is for $E_{rc} = 8.4$ mm day^{-1} and an irrigation interval of 7 days, yielding the estimate $K_{co} = 0.35$.

the average values of potential crop coefficients given in Table 4.4.5 to estimate monthly average evaporation rate from Eq. (4.4.19). However, in the case of repeatedly cut fodder crops, there will be dramatic shorter-term variations in evaporation during successive cut and regrowth cycles.

Other Irrigated Crops. Values of K_{co} for particular field crops with growth season extending over several seasons (e.g., bananas, sugarcane); values for deciduous fruit and nut crops (e.g., apples, cherries, peaches, apricots, pears, plums, walnuts, citrus, grapes, coffee, tea); and values for specialized crops, such as rice, have been tabulated by Doorenbos and Pruitt.[30] Readers interested in such crops are referred to that source.

TABLE 4.4.5 Recommended Average Values of Potential Crop Coefficient K_{co} for Successively Cut Fodder Crops and Grazed Pastures Which Are Well-Watered and Fertilized

	RH > 70%		RH < 30%	
	Wind, m s^{-1}		Wind, m s^{-1}	
	0–5	5+	0–5	5+
Fodder crops:				
Alfalfa	0.85	1.05	0.95	1.05
Grasses	0.80	1.00	0.90	1.00
Clover/grass-legumes	1.00	1.10	1.05	1.10
Pasture (grass, grass-legumes, alfalfa)	0.95	1.05	1.00	1.05

Source: Derived from Doorenbos and Pruitt (Ref. 30, Table 23). Used with permission.

For tall perennial fruit crops the size of K_{co} can be significantly influenced by agricultural practice, in particular the absence of a weed understory can lower K_{co} by 20 to 30 percent. Equally the use of sprinkler irrigation can alter the evaporation loss from tree crops, from significantly less than E_{rc} to greater than E_{rc}; see next section.

Forests. The evaporation rate from forests is more difficult to describe and estimate than for other vegetation types, and the reader is referred to Chap. 13 for greater detail. Most of this difficulty arises because turbulent diffusion in the atmosphere above forests is much more efficient than for other crops. For this reason the rate of evaporation when the canopy is wet can be very much greater than when it is dry (e.g., Refs. 108, 115). It is not therefore realistic to represent the average effect of controlling processes operating within the canopy in terms of a single (effective) surface resistance as in the case of the reference crop. It is necessary to consider transpiration and the evaporation of rainfall intercepted by forest canopy separately.

Perhaps in compensation for the more efficient turbulent diffusion, the surface resistance of forests tends to be higher, and transpiration rates are lower. Present evidence is not yet definitive but suggests[106,108] that the *transpiration rate* of well-watered forests is perhaps 80 ± 10 percent of reference crop evaporation [Eq. (4.4.14)] provided this has been calculated with the appropriate (forest) value of albedo; see Table 4.2.2.

The rate of evaporation of intercepted water from a wet canopy, on the other hand, commonly exceeds the potential evaporation rate for open water surfaces [Eq. (4.4.10)], and indeed often the energy locally available to support it. The additional energy is withdrawn from the atmosphere from warmer, drier air upwind. The net interception loss is typically 10 to 30 percent of rainfall, and depends partly on the amount of water which the canopy can store, i.e., *the interception storage capacity S;* but partly on the nature of the rainfall, in particular the intensity and duration of the rainstorms since up to half the evaporation occurs during the storm itself. For forests with complete canopy cover, intense, short-lived, convective storms, more common in tropical regions, are associated with a lower fractional interception loss of say 10 to 18 percent of precipitation[65,105,106] while storms associated with frontal rainfall, which may be less intense but last longer, tend to give a higher fractional interception loss of say 20 to 30 percent of precipitation.[23,42] For deciduous forests, the loss of leaves in winter reduces the fractional interception loss, typically by a factor of 2 to 3.

An approximate estimate of forest evaporation averaged over a month might therefore be made from

$$E^{\text{forest}} = 0.8\, E_{rc}^{\text{forest}} + \alpha_i P \qquad \text{mm day}^{-1} \tag{4.4.20}$$

where the first term is an estimate of transpiration, with E_{rc}^{forest} the value of reference crop evaporation rate calculated from Eq. (4.4.14) but with net radiation appropriate to a forest; and the second term is interception loss, with α_i the fractional interception loss (see previous paragraph for typical values). Equation (4.4.20) is (at best) accurate to 10 to 15 percent, depending on the accuracy of α_i, and is prone to overestimate evaporation rates. The estimate it gives should be limited to 0.9 R_n for extensive midcontinental forests or to R_n for less extensive forests within (say) 200 km of the sea.[106]

If detailed short-term rainfall data are available, it may be possible[40,42] to provide an improved estimate of the interception loss term in Eq. (4.4.20) from

$$\alpha_i P = \frac{0.95\, N_s\,(S + 0.2\,\tau_s)}{N_d} \qquad \text{mm day}^{-1} \tag{4.4.21}$$

where N_s is the number of storms in the averaging period of N_d days and τ_s is their average duration (in h), while S is the interception storage capacity of the canopy (in mm), with $S = 1.2$ mm typical for coniferous canopies and $S = 0.8$ mm typical of broadleaf canopies in full leaf.[106] Equation (4.4.21) implicitly assumes an evaporation rate of 0.2 mm h^{-1} during storms.[65] The factor 0.95 in Eq. (4.4.21) allows partly for the suppression of transpiration during rainstorms and partly for the possibility that a small proportion of storms[65] involve a total rainfall less than S.

4.4.7 Soil Moisture Restrictions

If estimates of evaporation are required for nonirrigated crops, the water status of the soil can be important, acting through the surface resistance. The value of K_c is reduced from K_{co} by including a factor $K_s(\theta)$ related to the volumetric soil moisture content θ:

$$E = K_c\, E_{rc} = K_s(\theta)\, K_{co}\, E_{rc} \qquad \text{mm day}^{-1} \tag{4.4.22}$$

The amount of accessible soil water available to the plants depends on their rooting depth, which can of course change as the vegetation grows, a point of particular significance for annual crops. The most realistic models of the soil water restriction on evaporation rate simulate plant extraction from a series of moisture stores arranged vertically above each other in the soil through the rooting zone.[34,85] They perform a running water balance for each moisture store, with some water (from rain or irrigation) infiltrating into the top store and draining from the bottom store; some moving between stores; and meanwhile some being extracted at each level in proportion to the product of E_{rc}, the fraction of root in each store, and a moisture extraction function $f(\theta)$.

Studies have been made of the variation in $f(\theta)$ in response to decreasing soil water: Dyck[33] lists the formulas given in Table 4.4.6. Results differ in detail, as might be expected for an empirical soil-related function of this type, but many workers (e.g., Refs. 34, 38, 39, 52, 85) are in broad agreement that the overall behavior during a drying cycle follows the general pattern illustrated in Fig. 4.4.3.

Soil *saturated* by rain or irrigation, with moisture content θ_s, first drains until the remaining water held by surface tension on the soil particles is in equilibrium with the gravitational forces causing drainage. It is then said to be at *field capacity,* with a moisture content θ_f. The drying proceeds with little soil moisture restriction until the soil moisture falls to θ_d, when the moisture content is typically 50 to 80 percent of θ_f; then the hydraulic conductivity K_s and the transpiration rate start to fall. They continue to fall until a *wilting point* is reached, where the soil moisture content is θ_w, and when, it is assumed, $K_s = 0$. This behavior seems to be similar for both crops and soil. In conditions of prolonged drought the crop begins to die and the evaporation rate is no longer controlled by meteorological conditions, but by soil characteristics, especially by hydraulic conductivity.

When modeling the change in evaporation in response to soil water status it is often convenient to work in terms of the soil water content, but plants are more sensitive to soil water potential ψ_s. Some of the variability in the functional form of $f(\theta)$ reported in the literature may therefore be caused by the variability in the relationship between θ_s and ψ_s for different soils. In some hydrologic applications the precise form of $f(\theta)$ is not too important. In particular, in the case of modeled water budgets the cumulative error in the calculated water store is set to zero each time the soil dries completely or when it is completely wetted by heavy rain.

TABLE 4.4.6 Recommended Forms of the Soil Moisture Stress Function $f(\theta)$ as cited by Dyck.[33] Used with permission.

Soil moisture stress function	Reference
Daily values	
$f(\theta) = [1 - \exp(-\gamma\theta)]\,[1 - 2\exp(-\gamma\theta_f) + \exp(-\gamma\theta)]^{-1}$	70
$f(\theta) = [1 + (\theta_c/\theta)^{bk}]^{-1}$; with $k = 2.69 \exp(-0.09\, E_{rc})^{-0.62}$	78
$f(\theta) = \left[\dfrac{(\theta - \theta_w)}{(\theta_f - \theta_w)}\right] F_s$	5
$f(\theta) = (1 - 0.533\, V)^{-1} \left[\dfrac{(\theta - \theta_w)}{(\theta_f - \theta_w)}\right]$	60
5-day values	
$f(\theta) = 0.2 + 2\left[\dfrac{(\theta - \theta_w)}{(\theta_f - \theta_w)}\right] - 1.2\left[\dfrac{(\theta - \theta_w)}{(\theta_f - \theta_w)}\right]^2$	93
Monthly values	
$f(\theta) = \left[\dfrac{(\theta - \theta_w)}{(\theta_f - \theta_w)}\right]$	21

where θ = soil moisture content (variable)
θ_w = soil moisture content when soil at "wilting point" ($E/E_{rc} = 0$)
θ_c = soil moisture content when $E/E_{rc} = 0.5$
θ_f = soil moisture content when soil at "field capacity"
V = vegetation canopy density
F_s = adjustment factor for functional form of Fig. 4.4.3

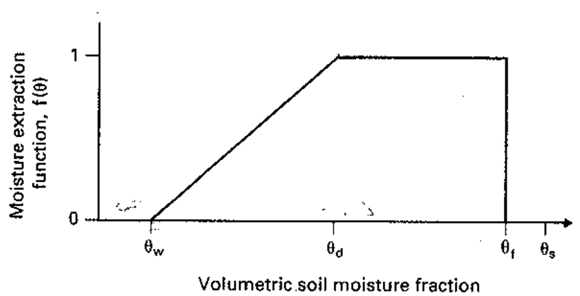

FIGURE 4.4.3 Typical variation of the moisture extraction function $f(\theta)$ which modifies the potential crop coefficient in response to changes in the volumetric soil moisture content θ in (portions of) the plants' rooting zone. θ_s, θ_f, and θ_w are the values of θ at saturation, field capacity, and wilting point, respectively, and (θ_d/θ_f) is typically 0.5 to 0.8. These values are determined by soil type.

4.4.8 Improving Evaporation Estimation

The adoption in this chapter of a reference crop evaporation rate which is precisely defined in terms of the physics of the evaporation process exploits research understanding gathered since the *Handbook of Applied Hydrology* was published in 1964. The significance of this development should not be underestimated in respect of the greater clarity and, on the basis of experimental evidence (e.g., Ref. 56), the improved accuracy it brings. At the same time the value of this step forward is compromised by the need to retain a "two-step" evaporation estimation procedure involving the poorly defined crop factor K_c, which has implicit meteorological dependence.

It is important that in punctuating the progress of hydrologic practice this *Handbook of Hydrology* should be a "semicolon," not a "full stop." With this in mind, I conclude with a recommendation. In order to provide a purer measure of crop control less contaminated by local climate, future field research into crop water requirements and the retrospective analysis of existing field data should seek to derive and report values of r_s^c, the effective average value of the surface resistance for the crop, rather than K_c.

If this becomes common practice, and in this way a relevant literature is created, then the author of this chapter in the next *Handbook of Hydrology* will be able to make a further significant step in advancing evaporation estimation practice by developing a "one-step" estimation procedure.

REFERENCES

1. Aboukhaled, A., A. Alfaro, and M. Smith, "Lysimeters," FAO Irrigation and Drainage Paper 39, Rome, 1982.
2. Allen, R. G., "A Penman for All Seasons," *J. Irrig. Drain. Eng.*, vol. 112, no. 4, pp. 348–368, 1986.
3. Allen, R. G., M. E. Jensen, J. L. Wright, and R. D. Burman, "Operational Estimates of Evapotranspiration," *Agron. J.*, vol. 81, pp. 650–662, 1989.
4. Allen, R. G., and W. O. Pruitt, "Rational Use of the FAO Blaney-Criddle Formula," *J. Irrig. Drain. Eng.*, vol. 112, no. IR2, pp. 139–155, 1986.
5. Baier, W., and G. W. Robertson, "A New Versatile Soil Moisture Budget," *Can. J. Plant Sci.*, vol. 46, pp. 299–315, 1966.
6. Baker, J. M., and C. H. M. Van Baval, "Measurement of Mass Flow of Water in the Stems of Herbaceous Plants," *Plant Cell Environ.*, vol. 10, pp. 777–782, 1987.
7. Bell, J. P., "A New Design Principle for Neutron Soil Moisture Gauges: The 'Wallingford' Neutron Probe," *Soil Sci.*, vol. 108, pp. 160–164, 1969.
8. Bell, J. P., "Neutron Probe Practice," *IH Report 19*, Institute of Hydrology, Wallingford, UK, 1987.
9. Bell, J. P., T. J. Dean, and M. G. Hodnett, "Soil Moisture Measurement by an Improved Capacitance Technique, part II: Field Techniques, Evaluation and Calibration," *J. Hydrol.*, vol. 93, pp. 79–90, 1987.
10. Black, T. A., and K. G. McNaughton, "Psychrometric Apparatus for Bowen Ratio Determination over Forests," *Boundary Layer Meteorol.*, vol. 2, pp. 246–254, 1971.
11. Blaney, H. F., and W. D. Criddle, "Determining Water Requirements in Irrigated Areas from Climatological and Irrigation Data," USDA (SCS) TP-96, p. 48, 1950.
12. Bouchet, R. J., "Evapotranspiration réelle et potentielle, signification climatique," in *Int. Assoc. Sci. Hydrol., Proceedings*, Berkeley, Calif., Symp. Publ. 62, pp. 134–142, 1963.

13. Bruin de, H. A. R., "A Model for the Priestley-Taylor Parameter," *J. Appl. Meteor.*, vol. 22, pp. 572–578, 1983.

14. Brunt, D., "Notes on Radiation in the Atmosphere," *Q. J. R. Meteorol. Soc.*, vol. 58, pp. 389–418, 1932.

15. Brutsaert, W., "Comments on Surface Roughness Parameters and the Height of Dense Vegetation," *J. Meteorol. Soc. Japan*, vol. 53, pp. 96–97, 1975.

16. Brutsaert, W., "Evaporation into the Atmosphere," D. Reidel Pub. Co., Dordrecht, Holland, 1982.

17. Brutsaert, W., and H. Stricker, "An Advection-Aridity Approach to Estimating Actual Regional Evaporation," *Water Resour. Res.*, vol. 15, pp. 443–450, 1979.

18. Brutsaert, W., and G. T. Yeh, "Evaporation from an Extremely Narrow Wet Strip at Ground Level," *J. Geophys. Res.*, vol. 74, pp. 3431–3433, 1969.

19. Brutsaert, W., and G. T. Yeh, "Implications of a Type of Empirical Evaporation Formula for Lakes and Pans," *Water Resour. Res.*, vol. 6, pp. 1202–1208, 1970.

20. Brutsaert, W., and S. L. Yu, "Mass Transfer Aspects of Pan Evaporation," *J. Appl. Meteorol.*, vol. 7, pp. 563–566, 1968.

21. Budyko, M., and L. I. Zubenok, "Opredelenie isparenija poverchnosti sushi," *AN SSSR Ser. Geogr.*, Booklet No. 6, 1961.

22. Calder, I. R., M. N. Narayanswamy, N. V. Srinivasalu, W. G. Darling, and A. J. Lardner, "Investigation into the Use of Deuterium as a Tracer for Measuring Transpiration from Eucalypts," *J. Hydrol.*, vol. 78, pp. 261–278, 1986.

23. Calder, I. R., and M. D. Newson, "Land Use and Upland Water Resources in Britain—A Strategic Look," *Water Resour. Bull.*, vol. 16, pp. 1628–1639, 1979.

24. Choudhury, B. L., and J. L. Monteith, "A Four-Layer Model for the Heat Budget of Homogeneous Land Surfaces," *Q. J. R. Meteorol. Soc.*, vol. 114, pp. 373–398, 1988.

25. Cohen, Y., G. C. Green, and M. Fuchs, "Improvement of the Heat Pulse Method for Determining Sap Flow in Trees," *Plant Cell Environ.*, vol. 4, pp. 425–431, 1987.

26. Coursey de, D. G., "The Goodwin Creek Research Catchment, Part I: Design Philosophy," *Proc. Symp. Hydrol. Res. Basins*, Bern, Sept. 21–23, 1982.

27. Crow, F. R., and S. D. Hottman, "Network Density of Temperature Profile Stations and Its Influence on the Accuracy of Lake Evaporation Calculations," *Water Resour. Res.*, vol. 9, pp. 895–899, 1973.

28. Dagg, M., "Evaporation Pans in East Africa," *Proc. Fourth Specialist Meeting on Applied Meteorology* in East Africa, Nairobi, 1968.

29. Dean, T. J., J. P. Bell, and A. J. B. Baty, "Soil Moisture Measurement by an Improved Capacitance Technique, Part I: Sensor Design and Performance," *J. Hydrol.*, vol. 93, pp. 67–78, 1987.

30. Doorenbos, J., and W. O. Pruitt, "Crop Water Requirements," *Irrigation and Drainage Paper*, 24, UN Food and Agriculture Organization, Rome, Italy, 1977.

31. Driedonks, A. G. M., "Dynamics of the Well-Mixed Atmospheric Boundary Layer," *Sci. Report W. R. 81-2*, K.N.M.I., de Bilt, The Netherlands, 1981.

32. Duffie, J. A., and W. A. Beckman, *Solar Engineering of Thermal Processes*, Wiley, New York, pp. 1–109, 1980.

33. Dyck, S., "Overview on the Present Status of the Concepts of Water Balance Models," *IAHS Publ.* 148, Wallingford, pp. 3–19, 1983.

34. Feddes, R. A., P. J. Kowalik, and H. Zaradny, "Simulation of Field Water Use and Crop Yield," *PUDOC*, Wageningen, 1978.

35. Frevert, D. K., R. W. Hill, and B. C. Braaten, "Estimation of FAO Evapotranspiration Co-efficients," *J. Irrig. Drain. Eng.*, vol. 109, no. IR2, pp. 265–270, 1983.

36. Fritschen, L. J., and J. R. Simpson, "Surface Energy and Radiation Balance Systems: General Description and Improvements," *J. Appl. Meteorol.*, vol. 28, pp. 680–689, 1989.

37. Gangopadhyaya, M., V. A. Uryvaev, M. H. Omar, T. J. Nordenson, and G. E. Harbeck, "Measurement and Estimation of Evaporation and Evapotranspiration," *WMO Technical Note*, no. 83, Geneva, Switzerland, 1966.

38. Gardner, W. R., and C. F. Ehlig, "The Influence of Soil Water on Transpiration of Plants," *J. Geophys. Res.*, vol. 68, pp. 5719–5724, 1963.

39. Gardner, W. R., and D. I. Hillel, "The Relation of External Evaporative Conditions to the Drying of Soils," *J. Geophys. Res.*, vol. 67, pp. 4319–4325, 1962.

40. Gash, J. H. C., "Comment on the Paper by A. S. Thom and H. R. Oliver, 'On Penman's Equation for Estimating Regional Evaporation'," *Q. J. R. Meteorol. Soc.*, vol. 104, pp. 532–533, 1978.

41. Gash, J. H. C., "A Note on Estimating the Effect of Limiting Fetch on Micrometeorological Evaporation Measurements," *Boundary Layer Meteorol.*, vol. 35, pp. 409–413, 1986.

42. Gash, J. H. C., I. R. Wright, and C. R. Lloyd, "Comparative Estimates of Interception Loss from Three Coniferous Forests in Great Britain," *J. Hydrol.*, vol. 48, pp. 89–105, 1980.

43. Greacon, E. L., ed., "Soil Water Assessment by the Neutron Method," CSIRO, Australia, 1981.

44. Halldin, S., and A. Lindroth, "Pine Forest Microclimate Simulation Using Different Diffusivities," *Boundary Layer Meteorol.*, vol. 35, pp. 103–123, 1986.

45. Ham, J. M., and J. L. Heilman, "Aerodynamic and Surface Resistances Affecting Energy Transport in a Sparse Crop," *Agric. For. Meteorol.*, vol. 53, pp. 267–284, 1991.

46. Harbeck, G. E., Jr, "A Practical Field Technique for Measuring Reservoir Evaporation Using Mass-Transfer Theory," *U.S. Geol. Surv. Prof. Paper*, 272-E, pp. 101–105, 1962.

47. Hargreaves, G. H., "Moisture Availability and Crop Production," *Trans. Am. Soc. Agric. Eng.*, vol. 18, no. 5, pp. 980–984, 1975.

48. Hargreaves, G. H., and Z. A. Samani, "Estimating Potential Evapotranspiration," Tech. Note, *J. Irrig. Drain Eng.*, vol. 108, no. 3, pp. 225–230, 1982.

49. Hargreaves, G. H., and Z. A. Samani, "Reference Crop Evapotranspiration from Temperature," *Appl. Eng. Agric.*, vol. 1, no. 2, pp. 96–99, 1985.

50. Hargreaves, G. L., G. H. Hargreaves, and J. P. Riley, "Agricultural Benefits for Senegal River Basin," *J. Irrig. Drain. Eng.*, vol. 111, no. 2, pp. 113–124, 1985.

51. Harrison, L. P., "Fundamental Concepts and Definitions Relating to Humidity," in A. Wexler, ed., *Humidity and Moisture*, vol. 3, Reinhold, New York, 1963.

52. Homes, R. M., "Discussion of 'A Comparison of Computed and Measured Soil Moisture under Snap Beans'," *J. Geophys. Res.*, vol. 66, pp. 3620–3622, 1961.

53. Idso, S. B., and R. D. Jackson, "Thermal Radiation from the Atmosphere," *J. Geophys. Res.*, vol. 74, pp. 5397–5403, 1969.

54. Itier, B., "Une méthode simplifée pour la mesure des flux de chaleur sensible," *Rech. Atmos.*, vol. 14, no. 1, pp. 17–34, 1980.

55. Itier, B., "Une méthode simple pour la mesure de l'evapotranspiration réelle a' l'echelle de la parcelle," *Agronomie*, vol. 1, no. 10, pp. 869–876, 1981.

56. Jensen, M. E., R. D. Burman, and R. G. Allen, "Evapotranspiration and Irrigation Water Requirements," *ASCE Manual* 70, p. 332, 1990.

57. Jones, H. G., *Plants and Microclimate*, Cambridge University Press, New York, 1984.

58. King, F. H., *Physics of Agriculture*, University of Wisconsin, Madison, Wis., 1910.

59. Kirby, C., and M. D. Newson, "The Plynlimon Catchments," *IH Report 109*, Institute of Hydrology, Wallingford, UK, 1990.

60. Koitzsch, R., and W. Golf, "Algorithmus zur Berechnung der realen Verdunstung, cited in 'Overview on the Present Status of the Concepts of Water Balance Models'," *IAHS Publ.* no. 148, Wallingford, pp. 3–19, 1983.

61. Lafleur, P. M., and W. R. Rouse, "Application of an Energy Combination Model for Evaporation from Sparse Canopies," *Agric. For. Meteorol.*, vol. 49, pp. 135–154, 1990.

62. Langbein, W. B., "Overview of AGU Chapman Conference on the Design of Hydrological Networks," *Water Resour. Res.*, vol. 15, no. 6, pp. 1867–1871, 1979.

63. Lhomme, J-P, "Extension of Penman's Formulae to Multi-Layer Models," *Boundary Layer Meteorol.*, vol. 42, pp. 281–291, 1988.

64. Lloyd, C. R., A. D. Culf, A. J. Dolman, and J. H. C. Gash, "Estimates of Sensible Heat Flux from Observations of Temperature Fluctuations," *Boundary Layer Meteorol.*, vol. 57, pp. 311–322, 1991.

65. Lloyd, C. R., J. H. C. Gash, W. J. Shuttleworth, and A. de O. Marques, "The Measurement and Modelling of Rainfall Interception by Amazonian Rainforest," *Agric. For. Meteorol.*, vol. 43, pp. 277–294, 1988.

66. Malhotra, G. P., and P. Bock, "Hydrologic Budget of North America and Sub-regions Formulated Using Atmospheric Vapor Flux Data," in *World Water Balance*, Studies and Reports in Hydrology, Report 11, UNESCO, Paris, 1972.

67. McNaughton, K. G., and T. W. Spriggs, "A Mixed-Layer Model for Regional Evaporation," *Boundary Layer Meteorol.*, vol. 34, pp. 243–263, 1986.

68. McNaughton, K. G., and T. W. Spriggs. "An Evaluation of the Priestley-Taylor Equation and the Complementary Relationship Using Results from a Mixed-Layer Model of the Convective Boundary Layer," *IAHS Publ.* no. 177, Wallingford, 1989.

69. McNeil, D. D., and W. J. Shuttleworth, "Comparative Measurements of Energy Fluxes over a Pine Forest," *Boundary Layer Meteorol.*, vol. 7, pp. 297–313, 1975.

70. Minhas, B. S., K. W. Parikh, and T. N. Srinavasan, "Toward the Structure of a Production Function for Wheat Yields with Dated Input of Irrigated Water," *Water Resour. Res.*, vol. 10, no. 3, pp. 383–393, 1974.

71. Monteith, J. L., "Evaporation and Surface Temperature," *Q. J. R. Meteorol. Soc.*, vol. 107, pp. 1–27, 1981.

72. Monteith, J. L., "Evaporation and the Environment," *Symp. Soc. Expl. Biol.*, vol. 19, pp. 205–234, 1965.

73. Morton, F. I., "Potential Evaporation and River Basin Evaporation," *J. Hydraul. Eng.*, vol. 91, no. HY6, pp. 67–97, 1965.

74. Morton, F. I., "Potential Evaporation as a Manifestation of Regional Evaporation," *Water Resour. Res.*, vol. 5, pp. 1244–1255, 1969.

75. Morton, F. I., "Estimating Evaporation and Transpiration from Climatological Observations," *J. Appl. Meteorol.*, vol. 14, pp. 488–497, 1975.

76. Morton, F. I., "Operational Estimates of Areal Evaporation and Their Significance to the Science and Practice of Hydrology," *J. Hydrol.*, vol. 66, pp. 1–76, 1983.

77. Nixon, P. R., and S. P. Lawless, "Translocation of Moisture with Time in Unsaturated Soil Profiles," *J. Geophys. Res.*, vol. 65, pp. 655–661, 1960.

78. Norero, A. L., "A Formula to Express Evapotranspiration as a Function of Soil Moisture and Evaporation Demands of the Atmosphere," Utah State University thesis, 1969.

79. Palmen, E., "Evaluation of Atmospheric Moisture Transport for Hydrological Purposes," *World Meteorological Organization IHD/Report* 1, International Hydrological Decade, 1967.

80. Penman, H. L., "Natural Evaporation from Open Water, Bare Soil and Grass," *Proc. R. Soc. London*, vol. A193, pp. 120–145, 1948.

81. Penman, H. L., *Vegetation and Hydrology*, Tech. Comm. 53, Commonwealth Bureau of Soils, Harpenden, England, 1963.

82. Penman, H. L., "Evaporation: An Introductory Survey," *Netherlands J. Agric. Sci.*, vol. 1, pp. 9–29, 87–97, 151–153, 1956.

83. Pereira, H. C., *Land Use and Water Resources in Temperate and Tropical Climates*, Cambridge University Press, 1973.

84. Pereira, H. C., *Policy and Practice in the Management of Tropical Watersheds*, Westview Press, Boulder, Colo., 1989.

85. Peschke, G., V. Dunger, and J. Gurtz, "Changes in Soil Moisture by Infiltration and Evapotranspiration," *IAHS Publ.* no. 156, 1986.

86. Priestley, C. H. B., and R. J. Taylor, "On the Assessment of Surface Heat Flux and Evaporation Using Large Scale Parameters," *Mon. Weather Rev.*, vol. 100, pp. 81–92, 1972.

87. Pruitt, W. O., "Prediction and Measurement of Crop Water Requirements: The Basis of Irrigation Scheduling," Faculty of Agriculture, University of Sydney, Sydney, NSW, 1986.

88. Pruitt, W. O., and J. Doorenbos, "Empirical Calibration, A Requisite for Evapotranspiration Formulae Based on Daily or Longer Mean Climatic Data?" *Proc. ICID International Round Table Conference on Evapotranspiration*, Budapest, Hungary, May 26–27, 1977.

89. Pruitt, W. O., and Lourence, F. J., "Experience in Lysimetry for ET and Surface Drag Measurements," in Advances in Evaporation, *ASAE Publ.* 14-85, American Society of Agricultural Engineers, St. Joseph, Mich., pp. 51–69, 1985.

90. Rao, K. S., J. C. Wyngaard, and O. R. Cote, "Local Advection of Momentum, Heat and Moisture in Micrometeorology," *Boundary Layer Meteorol.*, vol. 7, pp. 331–348, 1974.

91. Raphael, C., and J. E. Hay, "An Assessment of Models Which Use Satellite Data to Estimate Solar Irradiance at the Earth's Surface," *J. Clim. Appl. Meteorol.*, vol. 23, pp. 823–844, 1984.

92. Rasmussen, E. M., "Hydrological Application of Atmospheric Vapour-Flux Analyses," *WMO Operational Hydrology Report* 11, WMO-476, Geneva, Switzerland, 1977.

93. Renger, M., O. Strebel, and W. Giesel, "Beurteilung bodenkundlicher, kulturtechnischer und hydrolischer Fragen mit Hilfe von klimatischer Wasserbilanz und boden physikalischen Kennwerten," *Z. Kulturtech. Flurbereinig.*, vol. 15, pp. 148–160, 1974.

94. Roberts, J. M., "The Use of Tree Cutting Techniques in the Study of Water Relations of Mature *Pinus sylvestris L.*, Part I: The Technique and Survey of the Results," *J. Exp. Bot.*, vol. 28, pp. 751–767, 1977.

95. Robins, J. S., W. O. Pruitt, and W. H. Gardner, "Unsaturated Flow in Field Soils and Its Effect on Soil Moisture Investigations," *Soil Sci. Soc. Am. Proc.*, vol. 18, pp. 344–347, 1957.

96. Rodda, J. C., R. A. Downing, and F. M. Law, *Systematic Hydrology*, Butterworth, London, 1976.

97. Rodda, J. C., and S. W. Smith, "The Significance of the Systematic Error in Rainfall Measurement for Assessing Wet Deposition," *Atmos. Environ.*, vol. 20, pp. 1059–1064, 1986.

98. Rutter, A. J., K. A. Kershaw, P. C. Robins, and A. J. Morton, "A Predictive Model of Rainfall Interception in Forests. I: Derivation of the Model from Observations in a Plantation of Corsican Pine," *Agric. Meteorol.*, vol. 9, pp. 367–384, 1971.

99. Rutter, A. J., A. J. Morton, and P. C. Robins, "A Predictive Model of Rainfall Interception in Forests. II: Generalisation of the Model and Comparison with Observations in Some Coniferous and Hardwood Stands," *J. Appl. Ecol.*, vol. 12, pp. 367–380, 1975.

100. Sakuratani, T., "A Heat Balance Method for Measuring Water Flux in the Stem of Intact Plants," *J. Agric. Meteorol.*, vol. 37, no. 1, pp. 9–17, 1981.

101. Schuepp, P. H., M. Y. Leclerc, J. I. MacPherson, and R. L. Desjardin, "Footprint Prediction of Scalar Fluxes from Analytical Solutions of the Diffusion Equation," *Boundary Layer Meteorol.*, 1990.

102. Shuttleworth, W. J., "The Concept of Intrinsic Surface Resistance: Energy Budgets at a Partially Wet Surface," *Boundary Layer Meteorol.*, vol. 8, pp. 81–99, 1975.

103. Shuttleworth, W. J., "A Simplified One-Dimensional Theoretical Description of the Vegetation-Atmosphere Interaction," *Boundary Layer Meteorol.*, vol. 14, pp. 3–27, 1978.

104. Shuttleworth, W. J., "Macrohydrology—The New Challenge for Processes Hydrology," *J. Hydrol.*, vol. 100, pp. 31–56, 1988.

105. Shuttleworth, W. J., "Evaporation from Amazonian Rainforest," *Prof. R. Soc. London*, vol. B233, pp. 321–346, 1988.

106. Shuttleworth, W. J., "Micrometeorology of Temperate and Tropical Forest," *Phil. Trans. R. Soc. London*, vol. B324, pp. 299–334, 1989.

107. Shuttleworth, W. J., "Insight from Large-Scale Observational Studies of Land/Atmosphere Interactions," in Eric F. Wood, ed., "Land Surface Atmosphere Interactions: Parameterization and Analysis for Climate Modelling," *Surv. Geophys.*, vol. 12, pp. 3–39, 1990.

108. Shuttleworth, W. J., and I. R. Calder, "Has the Priestley-Taylor Equation Any Relevance to Forest Evaporation?" *J. Appl. Meteorol.*, vol. 18, pp. 634–638, 1979.

109. Shuttleworth, W. J., J. H. C. Gash, C. R. Lloyd, C. J. Moore, J. Roberts, A. de O. Marques, G. Fisch, V. de P. Silva Filho, M. N. G. Ribeiro, L. C. B. Molion, J. C. Nobre, L. D. A. de Sa, O. M. R. Cabral, S. R. Patel, and J. C. Mordas, "Observations of Radiation Exchange Above and Below Amazonian Rainforest," *Q. J. R. Meteorol. Soc.*, vol. 110, pp. 1163–1169, 1984.

110. Shuttleworth, W. J., J. H. C. Gash, C. R. Lloyd, D. D. McNeil, C. J. Moore, and J. S. Wallace, "An Integrated Micrometeorological System for Evaporation Measurement," *Agric. For. Meteorol.*, vol. 43, pp. 295–317, 1988.

111. Shuttleworth, W. J., and R. J. Gurney, "The Theoretical Relationship between Foliage," *Q. J. R. Meteorol. Soc.*, vol. 116, pp. 497–519, 1990.

112. Shuttleworth, W. J., and J. S. Wallace, "Evaporation from Sparse Crops—An Energy Combination Theory," *Q. J. R. Meteorol. Soc.*, vol. 111, pp. 839–855, 1984.

113. Sinclair, T. R., C. E. Murphy, and K. R. Knoerr, "Development and Evaluation of Simplified Models Simulating Canopy Photosynthesis and Transpiration," *J. Appl. Ecol.*, vol. 13, pp. 813–829, 1976.

114. Starr, V. P., and J. P. Peixoto, "On the Global Balance of Water Vapor and the Hydrology of Deserts," *Tellus*, vol. 10, pp. 188–194, 1958.

115. Stewart, J. B., "Evaporation from the Wet Canopy of a Pine Forest," *Water Resour. Res.*, vol. 13, no. 6, pp. 915–921, 1977.

116. Stewart, J. B., and A. S. Thom, "Energy Budgets in Pine Forest," *Q. J. R. Meteorol. Soc.*, vol. 99, pp. 154–170, 1973.

117. Tanner, C. B., "Measurement of Evapotranspiration," in *Irrigation of Agricultural Lands*, American Society of Agronomy Monograph 11, Madison, Wis., pp. 534–574, 1967.

118. Tetens, O., "Über einige meteorologische Begriffe," *Z. Geophys.*, vol. 6, pp. 203–204, 1930.

119. Thom, A. S., "Momentum, Mass and Heat Exchange of Vegetation," *Q. J. R. Meteorol. Soc.*, vol. 193, pp. 345–357, 1972.

120. Thom, A. S., "Momentum, Mass and Heat Exchange of Plant Communities," Sec. 3 in J. L. Monteith, ed., *Vegetation and the Atmosphere*, Academic Press, London, pp. 57–109, 1975.

121. Thom, A. S., and H. R. Oliver, "On Penman's Equation for Estimating Regional Evaporation," *Q. J. R. Meteorol. Soc.*, vol. 193, pp. 345–357, 1977.

122. Tillman, J. E., "The Indirect Determination of Stability, Heat and Momentum Fluxes in the Atmospheric Boundary Layer from Simple Scalar Variables During Dry, Unstable Conditions," *J. Appl. Meteorol.*, vol. 11, pp. 783–792, 1972.

123. Topp, G. C., J. L. Davis, and A. P. Annan, "Electromagnetic Determination of Soil-Water Content; Measurement in Coaxial Transmission Lines," *Water Resour. Res.*, vol. 16, pp. 574–582, 1980.

124. Topp, G. C., J. L. Davis, W. G. Bailey, and W. D. Zebchuk, "The Measurement of Soil Water Content Using a Portable TDR Hand Probe," *Can. J. Soils Sci.*, vol. 64, pp. 313–321, 1984.

125. Turc, L., "Evaluation des besoins en eau d'irrigation, evapotranspiration potentielle, formule climatique simplifice et mise a jour," *Ann. Agron.*, vol. 12, pp. 13–49, 1961.

126. Waggoner, P. E., *Vegetation and the Atmosphere*, vol. I, J. L. Monteith, ed., Academic Press, London, pp. 205–228, 1975.

127. Waggoner, P. E., and R. W. Reifsnyder, "Simulation of the Temperature Humidity and Evaporation Profiles in a Leaf Canopy," *J. Appl. Meteorol.*, vol. 7, pp. 400–409, 1968.

128. Waggoner, P. E., and N. C. Turner, "Comparison of Simulated and Actual Evaporation from Maize and Soil in a Lysimeter," *Agric. Meteorol.*, vol. 10, pp. 113–123, 1972.

129. Wesley, M. L., "Use of Variance Techniques to Measure Dry Air-Surface Exchange," *Boundary Layer Meteorol.*, vol. 44, pp. 13–31, 1988.

130. WMO, "Casebook on Hydrological Network Design Practice," *WMO Publ.* no. 324, Geneva, Switzerland, 1972.

131. WMO, "Hydrological Network Design and Information Transfer," *Operational Hydrology Report* 8, WMO Publ. 433, Geneva, Switzerland, 1976.

132. WMO, "Methods of Correction for Systematic Error in Point Precipitation Measurements for Operational Use," *Operational Hydrology Report* 21, WMO Publ. 589, Geneva, Switzerland, 1982.

133. Wright, I. R., "A Lysimeter for the Measurement of Evaporation from High Altitude Grass," in *Improved Methods of Hydrological Measurements in Mountain Areas*, IAHS Press, Wallingford, 1990.

134. Wright, J. L., "New Evapotranspiration Crop Co-efficients," *J. Irrig. Drain. Eng.*, vol. 108, no. IR2, pp. 57–74, 1982.

135. Wright, J. L., and M. E. Jensen, "Peak Water Requirements of (15) Crops in Southern Idaho," *J. Irrig. Drain. Eng.*, vol. 24, no. IR1, pp. 193–201, 1972.

136. Wyjk van, W. R., and D. A. de Vries, "Periodic Temperature Variations in Homogeneous Soil," in W. D. van Wijk, ed., *Physics of the Plant Environment*, North-Holland Publishing Co., Amsterdam, pp. 102–143, 1963.

137. Wyngaard, J. C., O. R. Cote, and Y. Izumi, "Local Free Convection, Similarity, and the Budgets of Shear Stress and Heat Flux," *J. Atmos. Sci.*, vol. 28, pp. 1171–1182, 1971.